The effect of molecular dissociation on the exchange-correlation Kohn-Sham potential.

Gritsenko, O.V.; Baerends, E.J.

published in
Physical Review A. Atomic, Molecular and Optical Physics
1996

DOI (link to publisher)
10.1103/PhysRevA.54.1957

document version
Publisher's PDF, also known as Version of record

Effect of molecular dissociation on the exchange-correlation Kohn-Sham potential

Oleg V. Gritsenko and Evert Jan Baerends
Afdeling Theoretische Chemie, Vrije Universiteit, De Boelelaan 1083, 1081 HV, Amsterdam, The Netherlands
(Received 2 May 1996)

The effect of molecular dissociation on the exchange-correlation Kohn-Sham potential v_{xc} has been studied by the construction of v_{xc} from the *ab initio* correlated density ρ for the monohydrides XH (X=Li, B) at several bond distances $R(X$—H). The molecular dissociation manifests itself in the formation of a characteristic peak of v_{xc} in the bonding region. The partially integrated conditional probability amplitude $\Phi(s_1,\vec{x}_2,\ldots,\vec{x}_N|\vec{r}_1)$ has been used to analyze the behavior of v_{xc} by means of a partitioning into various components: the potential of the exchange-correlation hole v_{xc}^{hole}, the kinetic component $v_{c,kin}$, and the ''response'' component v_{resp}. These components have been constructed from *ab initio* correlated first- and second-order density matrices. The peak of v_{xc} in the bonding region has been represented as a combination of the corresponding peak of $v_{c,kin}$ and the positive buildup of v_{resp} around the more electronegative atom H. Using the conditional amplitude analysis, the asymptotical expressions have been obtained for v_{resp} and its positive buildup for the general case of a heteroatomic molecule AB. The dependence of the Kohn-Sham energy characteristics such as the kinetic energy of noninteracting particles T_s, the kinetic part of the exchange-correlation energy T_c, and the energy of the highest occupied molecular orbital ϵ_N on the bond distance has been studied. The results obtained have been compared with those for the homoatomic two-electron H_2 molecule. [S1050-2947(96)03109-5]

PACS number(s): 31.15.Ew

I. INTRODUCTION

Construction of the exchange-correlation Kohn-Sham (KS) potential v_{xc} and orbitals $\{\phi_i\}$ from the correlated *ab initio* electron density ρ of an N-electron system becomes a promising field within density-functional theory (DFT). Starting with the simple special case of the two-electron atomic systems [1] (and, more recently [2,3]), examples of v_{xc} were subsequently constructed for the three-electron Li atom and light closed-shell atoms Be and Ne [4–10], and then for all atoms He through Ar [11,12].

The construction of v_{xc} was extended to molecules, starting also with the special case of the two-electron H_2 molecule [2]. Then, v_{xc} was constructed for LiH [13] and for BH, HF, and N_2 [14,15]. In [2,16] a partitioning scheme was proposed for the analysis of v_{xc}, which is based on the partially integrated conditional probability amplitude $\Phi(s_1,\vec{x}_2,\ldots,\vec{x}_N|\vec{r}_1)$ [17] of the total ground-state wave function $\Psi_0(\vec{x}_1,\vec{x}_2,\ldots,\vec{x}_N)$. Various components of v_{xc} are obtained within this scheme from ρ and also from the correlated first- and second-order density matrices $\rho(\vec{r}_1',\vec{r}_1)$ and $\rho_2(\vec{r}_1,\vec{r}_2)$. Using a combination of some components of v_{xc} a scheme of construction of the exchange-correlation energy density ϵ_{xc} from $\rho,\rho(\vec{r}_1',\vec{r}_1)$ and $\rho_2(\vec{r}_1,\vec{r}_2)$ was proposed in [18] and examples of ϵ_{xc} were obtained for He, H_2 [2] and also for LiH, BH, HF [15].

One of the key problems of the molecular KS theory is the effect of various molecular processes on the KS characteristics. The simplest unimolecular process is the dissociation of a diatomic molecule and an interesting topic is the evolution of the KS energy characteristics and the shape of v_{xc} with increasing bond distance. Hitherto, v_{xc} has been constructed for the diatomic molecules only at their equilibrium bond lengths R_e. The only exception is the special case of the homoatomic two-electron H_2 molecule, for which the KS solution was obtained in a straightforward way from ρ at several distances R(H—H) [2]. As a matter of fact, even in the latter case the total v_{xc} has not been presented, only its various components.

In this paper the effect of molecular dissociation on v_{xc} is investigated by comparison of v_{xc} and its components constructed from *ab initio* first- and second-order density matrices for the heteroatomic molecules LiH and BH at several bond distances $R(X$—H). Specific dissociation effects for the heteroatomic molecules, in particular, the positive buildup of v_{xc} around the more electronegative atom are established and interpreted in terms of the partially integrated conditional probability amplitude $\Phi(s_1,\vec{x}_2,\ldots,\vec{x}_N|\vec{r}_1)$. The dependence of the KS energy characteristics such as the kinetic energy of noninteracting particles T_s, the kinetic part of the correlation energy T_c, and the energy of the highest occupied molecular orbital (HOMO) ϵ_N on the bond distance is investigated. The results for the heteroatomic molecules are compared with those for the H_2 molecule.

II. PARTITIONING OF v_{xc}

The Kohn-Sham exchange-correlation potential $v_{xc}([\rho];\vec{r})$ is a part of the total KS potential $v_s([\rho];\vec{r})$

$$\{-\tfrac{1}{2}\nabla^2+v_s(\vec{r})\}\phi_i(\vec{r})=\epsilon_i\phi_i(\vec{r}), \tag{1}$$

$$\sum_{i=1}^{N}|\phi_i(\vec{r})|^2=\rho(\vec{r}), \tag{2}$$

or, more precisely, a component of the potential arising from the two-particle electron interaction $v_{el}([\rho];\vec{r})$

$$v_s(\vec{r})=v_{ext}(\vec{r})+v_{el}(\vec{r}), \tag{3}$$

$$v_{\mathrm{el}}(\vec{r})=v_{\mathrm{H}}(\vec{r})+v_{\mathrm{xc}}(\vec{r}), \tag{4}$$

which represents the local effect of electron exchange and Coulomb correlation in the one-electron KS equations (1). Here v_{ext} is the external potential, v_{H} is the Hartree potential of the electrostatic electron repulsion, N is the number of electrons in the system and the occupied KS orbitals ϕ_i yield the total electron density ρ via Eq. (2). $v_{\mathrm{xc}}([\rho];\vec{r})$ is defined in DFT as the functional derivative of the exchange-correlation energy $E_{\mathrm{xc}}[\rho]$ with respect to $\rho(\vec{r})$

$$v_{\mathrm{xc}}([\rho];\vec{r})=\frac{\delta E_{\mathrm{xc}}[\rho]}{\delta\rho(\vec{r})}. \tag{5}$$

For the results of this paper it is essential to use the partitioning [2] of v_{xc} in terms of the conditional probability amplitude $\Phi(s_1,\vec{x}_2,\ldots,\vec{x}_N|\vec{r}_1)$ [17] of the total ground-state wave function $\Psi_0(\vec{x}_1,\vec{x}_2,\ldots,\vec{x}_N)$ ($\{\vec{x}_i\}=\{\vec{r}_i,s_i\}$, $\{\vec{r}_i\}$ are the space and $\{s_i\}$ are the spin variables)

$$\Phi(s_1,\vec{x}_2,\ldots,\vec{x}_N|\vec{r}_1)=\frac{\Psi_0(\vec{x}_1,\ldots,\vec{x}_N)}{\sqrt{\rho(\vec{r}_1)/N}}. \tag{6}$$

$\Phi(s_1,\vec{x}_2,\ldots,\vec{x}_N|\vec{r}_1)$ embodies all effects of electron correlation (exchange as well as Coulomb) in that its square is the probability distribution of the remaining $N-1$ electrons associated with positions $\vec{x}_2,\ldots,\vec{x}_N$ when one electron is known to be at $\vec{r}_1$. One can define also the conditional probability amplitude $\Phi_s(s_1,\vec{x}_2,\ldots,\vec{x}_N|\vec{r}_1)$ of the one-determinantal wave function $\Psi_s(\vec{x}_1,\vec{x}_2,\ldots,\vec{x}_N)$ built from the occupied KS orbitals $\phi_i(\vec{r}_i)$

$$\Phi_s(s_1,\vec{x}_2,\ldots,\vec{x}_N|\vec{r}_1)=\frac{\Psi_s(\vec{x}_1,\ldots,\vec{x}_N)}{\sqrt{\rho(\vec{r}_1)/N}}. \tag{7}$$

To partition v_{xc} according to [2], one has to start with the stationary N-electron Schrödinger equations for $\Psi(\vec{x}_1,\vec{x}_2,\ldots,\vec{x}_N)$ and $\Psi_s(\vec{x}_1,\vec{x}_2,\ldots,\vec{x}_N)$

$$H^N\Psi_0=E_0^N\Psi_0, \tag{8}$$

$$H_s^N\Psi_s=E_s^N\Psi_s \tag{9}$$

and partition the corresponding Hamiltonians as

$$H^N=-\frac{1}{2}\nabla_1^2+v_{\mathrm{ext}}(\vec{r}_1)+\sum_{j=2}^{N}\frac{1}{|\vec{r}_1-\vec{r}_j|}+H^{N-1}, \tag{10}$$

$$H^{N-1}=\sum_{j=2}^{N}\left\{-\frac{1}{2}\nabla_j^2+v_{\mathrm{ext}}(\vec{r}_j)+\sum_{k>j}^{N}\frac{1}{|\vec{r}_j-\vec{r}_k|}\right\}, \tag{11}$$

$$H_s^N=-\frac{1}{2}\nabla_1^2+v_{\mathrm{ext}}(\vec{r}_1)+v_{\mathrm{el}}(\vec{r}_1)+H_s^{N-1}, \tag{12}$$

$$H_s^{N-1}=\sum_{j=2}^{N}\left\{-\frac{1}{2}\nabla_j^2+v_{\mathrm{ext}}(\vec{r}_j)+v_{\mathrm{el}}(\vec{r}_j)\right\}. \tag{13}$$

Inserting (6), (7), and (10)–(13) into (8) and (9), we get

$$\left[-\frac{1}{2}\nabla_1^2+v_{\mathrm{ext}}(\vec{r}_1)+\sum_{j=2}^{N}\frac{1}{|\vec{r}_1-\vec{r}_j|}+H^{N-1}\right]\sqrt{\rho(\vec{r}_1)/N}\,\Phi(s_1,\vec{x}_2,\ldots,\vec{x}_N|\vec{r}_1)=E_0^N\sqrt{\rho(\vec{r}_1)/N}\,\Phi(s_1,\vec{x}_2,\ldots,\vec{x}_N|\vec{r}_1), \tag{14}$$

$$\left[-\frac{1}{2}\nabla_1^2+v_{\mathrm{ext}}(\vec{r}_1)+v_{\mathrm{el}}(\vec{r}_1)+H_s^{N-1}\right]\times\sqrt{\rho(\vec{r}_1)/N}\,\Phi_s(s_1,\vec{x}_2,\ldots,\vec{x}_N|\vec{r}_1)=E_s^N\sqrt{\rho(\vec{r}_1)/N}\,\Phi_s(s_1,\vec{x}_2,\ldots,\vec{x}_N|\vec{r}_1). \tag{15}$$

To obtain one-electron equations, both sides of Eqs. (14) and (15) are multiplied by $\Phi^*(s_1,\vec{x}_2,\ldots,\vec{x}_N|\vec{r}_1)$ and $\Phi_s^*(s_1,\vec{x}_2,\ldots,\vec{x}_N|\vec{r}_1)$, respectively, and integrated over the coordinates $s_1,\vec{x}_2,\ldots,\vec{x}_N$. Then, the ground-state energy E_0^{N-1} of the $(N-1)$ electron system with the same external potential $v_{\mathrm{ext}}(\vec{r})$ is subtracted from both sides of Eq. (14), while the analogous KS energy E_s^{N-1}

$$E_s^{N-1}=\int\Psi_s^{N-1}{}^*(\vec{x}_2,\ldots,\vec{x}_N)H_s^{N-1}\Psi_s^{N-1}\times(\vec{x}_2,\ldots,\vec{x}_N)d\vec{x}_2\cdots d\vec{x}_N \tag{16}$$

is subtracted from both sides of Eq. (15). Here the $(N-1)$ electron *KS* determinant Ψ_s^{N-1} is generated from the N electron *KS* determinantal wave function Ψ_s defined above by the annihilation of one electron from the highest occupied orbital ϕ_N. After these operations, making use of the normalization properties of the conditional amplitudes

$$\int\Phi^*(s_1,\vec{x}_2,\ldots,\vec{x}_N|\vec{r}_1)\Phi(s_1,\vec{x}_2,\ldots,\vec{x}_N|\vec{r}_1)ds_1d\vec{x}_2\cdots d\vec{x}_N=1, \tag{17}$$

$$\int\Phi_s^*(s_1,\vec{x}_2,\ldots,\vec{x}_N|\vec{r}_1)\Phi_s(s_1,\vec{x}_2,\ldots,\vec{x}_N|\vec{r}_1)ds_1d\vec{x}_2\cdots d\vec{x}_N=1, \tag{18}$$

one can obtain from (14) and (15) two equivalent forms of the Euler-Lagrange equation for the square root of the electron density

$$\left\{-\frac{1}{2}\nabla^2+v_{\mathrm{ext}}(\vec{r})+v_{\mathrm{H}}(\vec{r})+v_{\mathrm{xc}}^{\mathrm{hole}}(\vec{r})+v_{\mathrm{kin}}(\vec{r})+v^{N-1}(\vec{r})\right\}\times\sqrt{\rho(\vec{r})}=\mu\sqrt{\rho(\vec{r})}, \tag{19}$$

$$\left\{-\frac{1}{2}\nabla^2+v_{\mathrm{ext}}(\vec{r})+v_{\mathrm{H}}(\vec{r})+v_{\mathrm{xc}}(\vec{r})+v_{s,\mathrm{kin}}(\vec{r})+v_s^{N-1}(\vec{r})\right\}\times\sqrt{\rho(\vec{r})}=\mu\sqrt{\rho(\vec{r})}, \tag{20}$$

where $\mu=E_0^N-E_0^{N-1}$ is the first vertical ionization energy of the system, which in its turn is equal to the energy of the highest occupied orbital $\mu=\epsilon_N=E_s^N-E_s^{N-1}$.

In Eq. (19) $v_{\rm xc}^{\rm hole}$, $v_{\rm kin}$, and v^{N-1} are the local potentials obtained from the partially integrated conditional amplitude $\Phi(s_1,\vec{x}_2,\ldots,\vec{x}_N|\hat{r}_1)$, which represent various characteristics of the electron correlation. $v_{\rm xc}^{\rm hole}$ is the potential of the exchange-correlation hole

$$\begin{aligned} v_{\rm xc}^{\rm hole}(\vec{r}_1)&=\int \Phi^*(s_1,\vec{x}_2,\ldots,\vec{x}_N|\vec{r}_1)\\ &\quad\times\left[\sum_{j=2}^{N}\frac{1}{|\vec{r}_1-\vec{r}_j|}\right]\Phi(s_1,\vec{x}_2,\ldots,\vec{x}_N|\vec{r}_1)\\ &\quad\times ds_1 d\vec{x}_2\cdots d\vec{x}_N-v_{\rm H}(\vec{r})\\ &=\int\frac{\rho_2(\vec{r}_1,\vec{r}_2)-\rho(\vec{r}_1)\rho(\vec{r}_2)}{|\vec{r}_1-\vec{r}_2|\rho(\vec{r}_1)}\,d\vec{r}_2\\ &=\int\frac{\rho(\vec{r}_2)[g(\vec{r}_1,\vec{r}_2)-1]}{|\vec{r}_1-\vec{r}_2|}\,d\vec{r}_2, \end{aligned}\tag{21}$$

where $\rho_2(\vec{r}_1,\vec{r}_2)$ and $g(\vec{r}_1,\vec{r}_2)$ are the diagonal part of the second-order density matrix and the pair-correlation function with the electron interaction λ/r_{12} at full strength $\lambda=1$. $v_{\rm kin}$ is the kinetic component

$$\begin{aligned} v_{\rm kin}(\vec{r}_1)&=\frac{1}{2}\int|\nabla_1\Phi(s_1,\vec{x}_2,\ldots,\vec{x}_N|\vec{r}_1)|^2 ds_1 d\vec{x}_2\cdots d\vec{x}_N\\ &=\frac{\nabla_{1'}\nabla_1\rho(\vec{r}_1{}',\vec{r}_1)|_{\vec{r}_1{}'=\vec{r}_1}}{2\rho(\vec{r}_1)}-\frac{[\nabla\rho(\vec{r}_1)]^2}{8\rho^2(\vec{r}_1)}, \end{aligned}\tag{22}$$

where $\rho(\vec{r}_1{}',\vec{r}_1)$ is the first-order density matrix. $v_{\rm kin}$ reflects the magnitude of change in Φ with changing $\vec{r}_1$ (so it is a measure of the *change* in the correlation hole with variations of the reference position $\vec{r}_1$). $v^{N-1}(\vec{r})$ is the energy expectation value $E^{N-1}(\vec{r})$ of the system of $(N-1)$ electrons described by the conditional amplitude

$$\begin{aligned} E^{N-1}(\vec{r}_1)&=\int\Phi^*(s_1,\vec{x}_2,\ldots,\vec{x}_N|\vec{r}_1)H^{N-1}\Phi\\ &\quad\times(s_1,\vec{x}_2,\ldots,\vec{x}_N|\vec{r}_1)ds_1 d\vec{x}_2\cdots d\vec{x}_N \end{aligned}\tag{23}$$

minus the ground-state energy of the $(N-1)$ electron system E_0^{N-1}

$$v^{N-1}(\vec{r})=E^{N-1}(\vec{r})-E_0^{N-1}.\tag{24}$$

The potentials $v_{s,\rm kin}$ and v_s^{N-1} are obtained, in complete analogy with $v_{\rm kin}$ and v^{N-1}, from the KS conditional amplitude $\Phi_s(s_1,\vec{x}_2,\ldots,\vec{x}_N|\vec{r}_1)$. Due to the simple one-electron nature of H_s^{N-1} and Ψ_s, they can be expressed explicitly in terms of the KS orbitals and orbital energies as [16,19]

$$\begin{aligned} v_{s,\rm kin}(\vec{r}_1)&=\frac{1}{2}\int|\nabla_1\Phi_s(s_1,\vec{x}_2,\ldots,\vec{x}_N|\vec{r}_1)|^2 ds_1 d\vec{x}_2\cdots d\vec{x}_N\\ &=\frac{1}{2}\sum_{i=1}^{N}\left|\nabla_1\frac{\phi_i(\vec{r}_1)}{\rho^{1/2}(\vec{r}_1)}\right|^2, \end{aligned}\tag{25}$$

$$\begin{aligned} v_s^{N-1}(\vec{r}_1)&=\int\Phi_s^*(s_1,\vec{x}_2,\ldots,\vec{x}_N|\vec{r}_1)H_s^{N-1}\Phi_s\\ &\quad\times(s_1,\vec{x}_2,\ldots,\vec{x}_N|\vec{r}_1)ds_1 d\vec{x}_2\cdots d\vec{x}_N-E_s^{N-1}\\ &=\mu-\sum_{i=1}^{N}\epsilon_i\frac{|\phi_i(\vec{r}_1)|^2}{\rho^{1/2}(\vec{r}_1)}. \end{aligned}\tag{26}$$

Equations (19) and (20) provide a partitioning of $v_{\rm xc}$ in terms of the above-mentioned potentials. Equating the left-hand sides of (19) and (20) leads to the following expression for $v_{\rm xc}$:

$$v_{\rm xc}(\vec{r})=v_{\rm xc}^{\rm hole}(\vec{r})+v_{c,\rm kin}(\vec{r})+v^{N-1}(\vec{r})-v_s^{N-1}(\vec{r}),\tag{27}$$

where

$$v_{c,\rm kin}(\vec{r})=v_{\rm kin}(\vec{r})-v_{s,\rm kin}(\vec{r}).\tag{28}$$

As was shown in [16], the potentials v^{N-1} and v_s^{N-1} can be also expressed in terms of the ''response'' potentials

$$v^{N-1}(\vec{r})=v_{\rm xc}^{\rm hole,resp}(\vec{r})+v_{\rm kin}^{\rm resp}(\vec{r}),\tag{29}$$

$$v_s^{N-1}(\vec{r})=v_{s,\rm kin}^{\rm resp}(\vec{r}).\tag{30}$$

Here the potential $v_{\rm xc}^{\rm hole,resp}$ is an integral of the linear ''response'' of $g([\rho];\vec{r}_1,\vec{r}_2)$, $\delta g([\rho];\vec{r}_1,\vec{r}_2)/\delta\rho(\vec{r}_3)$

$$v_{\rm xc}^{\rm hole,resp}([\rho];\vec{r}_3)=\frac{1}{2}\int\frac{\rho(\vec{r}_1)\rho(\vec{r}_2)}{|\vec{r}_1-\vec{r}_2|}\frac{\delta g([\rho];\vec{r}_1,\vec{r}_2)}{\delta\rho(\vec{r}_3)}\,d\vec{r}_1 d\vec{r}_2.\tag{31}$$

It is a measure of the sensitivity of the pair-correlation function to density variations. These density variations may be understood in the following way. If the density changes to (v representable) $\rho+\delta\rho$, then according to the Hohenberg-Kohn theorem this changed density corresponds uniquely to an external potential $v_{\rm ext}+\delta v_{\rm ext}$. For the system with external potential $v_{\rm ext}+\delta v_{\rm ext}$ we have the corresponding Kohn-Sham system and the pair-correlation function $g([\rho+\delta\rho];\vec{r}_1,\vec{r}_2)$. So the derivative occurring in the response potential (31) may be regarded as the linear response of g to density change $\delta\rho$ caused by potential change $\delta v_{\rm ext}$. $v_{\rm kin}^{\rm resp}$ and $v_{s,\rm kin}^{\rm resp}$ are the response of the potentials $v_{\rm kin}$ and $v_{s,\rm kin}$ to density variations

$$v_{\rm kin}^{\rm resp}([\rho];\vec{r}_1)=\int\rho(\vec{r}_2)\frac{\delta v_{\rm kin}([\rho];\vec{r}_2)}{\delta\rho(\vec{r}_1)}\,d\vec{r}_2,\tag{32}$$

$$v_{s,\rm kin}^{\rm resp}([\rho];\vec{r}_1)=\int\rho(\vec{r}_2)\frac{\delta v_{s,\rm kin}([\rho];\vec{r}_2)}{\delta\rho(\vec{r}_1)}\,d\vec{r}_2.\tag{33}$$

The expressions (32) and (33) are obtained from the comparison of Eq. (27) for $v_{\rm xc}$ with its definition (5) as a functional derivative of $E_{\rm xc}[\rho]$. Since the difference between v^{N-1} and v_s^{N-1} accumulates all the response terms, we shall use for it the notation $v_{\rm resp}$

$$v_{\rm resp}(\vec{r})=v^{N-1}(\vec{r})-v_s^{N-1}(\vec{r}),\tag{34}$$

so that finally we get for $v_{\rm xc}$ the expression

$$v_{\rm xc}(\vec{r}) = v_{\rm xc}^{\rm hole}(\vec{r}) + v_{c,\rm kin}(\vec{r}) + v_{\rm resp}(\vec{r}). \tag{35}$$

It should be noted that the leading term of $v_{\rm xc}$ is the hole potential $v_{\rm xc}^{\rm hole}$. It has been demonstrated that this is, in most regions, the most important part of $v_{\rm xc}$ indeed [2,18,15]. The fact that the KS potential v_s incorporates in addition to the potential of the Fermi hole also the potential of the Coulomb hole distinguishes it from the effective potential in the one-electron Hartree-Fock equations which only contains an (orbital dependent) Fermi-hole contribution. There are many cases where the Hartree-Fock electron density differs strongly from the exact density. Examples are H_2 at large distance, and N_2 and MnO_4^- at equilibrium distance [20]. This is caused primarily by the lack of a Coulomb-hole-potential contribution in the Hartree-Fock potential. In the case of MnO_4^- it has been demonstrated [21] that for this reason the Hartree-Fock orbitals are rather distorted, yielding an erroneous heteropolar character to the metal-ligand bond and wrong d-electron counts when compared to configuration interaction (CI) and complete active space self-consistent field (CASSCF) calculations. The KS orbitals, however, do reflect the homopolar nature of the bonds and lead to d-electron counts in agreement with the CASSCF calculations. Quite generally it may be argued that, because of the good physics present in the components of the KS potential, the KS orbitals are in no way ''inferior'' to, e.g., Hartree-Fock orbitals and, in fact, may well be more reliable in qualitative molecular orbital (MO) considerations [22].

In the next section we shall use the presented partitioning scheme and, in particular, formulas for v^{N-1} and v_s^{N-1} in order to establish and to interpret the features of $v_{\rm xc}$ which arise in the course of the dissociation of a heteroatomic molecule.

III. ORIGIN OF THE POSITIVE BUILDUP OF $v_{\rm xc}$ AROUND A MORE ELECTRONEGATIVE ATOM OF A SYSTEM AB

Dissociation of the heteroatomic bond A—B produces a spectacular effect on the Kohn-Sham potential v_s, namely, a positive buildup of v_s around the more electronegative atom B [23,24]. This can be illustrated with the simple example of two interacting model ''one-dimensional hydrogenlike atoms'' [24]. A single electron of the model ''atom'' is bound to the external δ function potential $v_{\rm ext}(x) = -a\,\delta(x)$, so that the ''atomic'' orbital is $\phi_A(x) = \sqrt{a}\,\exp(-a|x|)$ and the ionization energy I_A is $a^2/2$. The single KS orbital of the closed-shell system AB is constructed as the bonding orbital

$$\phi(x) = c[\sqrt{a}e^{-a|x|} + \sqrt{b}e^{-b|x-l|}], \tag{36}$$

where l is the bond length and c normalizes the total density $\rho(x) = 2\phi^2(x)$ to two electrons. At large distance l this construction correctly yields a sum of the ''atomic'' densities for $\rho(x)$. The energy ϵ of $\phi(x)$ is equal to minus the ionization energy of the system, which at large l values is equal to that of the less electronegative atom A, $\epsilon = -a^2/2$.

Figure 1 represents the KS potential $v_s(x)$ of the system AB obtained for $l=3$, $l=7$ a.u. and $x \neq x_A$, $x \neq x_B$ with the insertion of (36) and $-I_A = -a^2/2$ into the one-electron KS equation

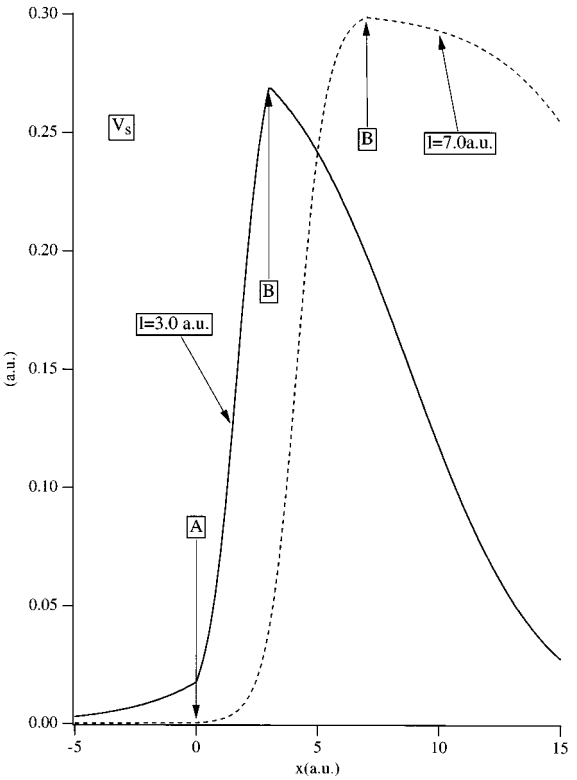

FIG. 1. Kohn-Sham potential for the model one-dimensional two-electron system AB.

$$-\frac{1}{2}\frac{d^2\phi(x)}{dx^2} + v_s(x)\,\phi(x) = \epsilon\phi(x). \tag{37}$$

The parameter values $a=0.63$ and $b=1.0$ a.u. were chosen in order to fit the ionization energies [25] of the atoms Li and H, respectively. One can see from Fig. 1 a distinct positive buildup of $v_s(x)$ around the more electronegative atom B. While in the region between A and B $v_s(x)$ has a similar form for both distances l, it differs in the outer region beyond the B ''atom.'' In this latter region $v_s(x)$ gradually decreases for $l=3$ a.u. and it forms a rather sharp ''peak'' around B. On the other hand, for $l=7$ a.u it has a much more shallow form and forms a ''step'' with the B ''atom'' being on its upper part. With increasing l the maximum of $v_s(x)$ approaches the value 0.302 a.u. of the difference $I_B - I_A$ of the ionization energies.

Qualitative arguments were put forward in [23] and [24] to demonstrate that v_s exhibits a similar positive shift

$$\Delta v_s \approx I_B - I_A \tag{38}$$

in the general case of the real three-dimensional heteroatomic system AB at large bond distances. In [24] the principle of equalization of the KS orbital energies for the fragments A and B was used and discontinuities of the derivative of the total energy E as a function of the particle number $(N+\omega)$ were explored. In [23] arguments concerning the asymptotic behavior in different regions of the highest occupied MO (HOMO) were used to show (38). In [23] the positive buildup was attributed to the exchange-correlation part $v_{\rm xc}$ of v_s.

In this paper we establish the existence of the positive buildup of v_{xc} around the more electronegative atom B of a system AB directly from the total many-electron wave function $\Psi(\vec{x}_1,\ldots,\vec{x}_N)$ of the system. Based on the partitioning of v_{xc} in Sec. II we shall demonstrate that this buildup originates in the response part v_{resp} of v_{xc} and we shall derive an expression for it, making use of the conditional probability amplitude $\Phi(s_1,\vec{x}_2,\ldots,\vec{x}_N|\vec{r}_1)$ [Eq. (6)].

We start with the definition (34) of $v_{resp}(\vec{r}_1)$ and we shall analyze the form of $v_{resp}(\vec{r}_1)$ in the region of the highest occupied MO (HOMO) $\phi_N(\vec{r}_1)$. It follows from (26) that $v_s^{N-1}(\vec{r}_1)$ in this region vanishes, since $\phi_N(\vec{r}_1)$ constitutes the dominant contribution to $\rho(\vec{r}_1)$, so that $v_{resp}(\vec{r}_1)$ reduces effectively to $v^{N-1}(\vec{r}_1)$

$$v_{resp}(\vec{r}_1)\approx v^{N-1}(\vec{r}_1)=E^{N-1}(\vec{r}_1)-E_0^{N-1}, \tag{39}$$

which, according to (23), (24), is determined by the function $\Phi(s_1,\vec{x}_2,\ldots,\vec{x}_N|\vec{r}_1)$.

Suppose that the reference electron is in the region Ω_B of the more electronegative atom B, $\vec{r}_1\in\Omega_B$. In this case the conditional amplitude $\Phi(s_1,\vec{x}_2,\ldots,\vec{x}_N|\vec{r}_1)$ describes the $(N-1)$-electron system $A—B^+$ consisting of the neutral atom A interacting with a cation B^+. This cation will not in general be in the ground state of the B^+ system, but if $\vec{r}_1$ is actually at significant distance from the electronic cloud of B^+, although still by assumption much closer to B than to A, it has been established by Katriel and Davidson [26] that B^+ is in that case in its ground state. So in that case at large bond distances $R(A—B)$ the energy of this system reduces to

$$E(A-B^+)\approx E_0(A)+E_0(B)+I_B+E_{int}(A-B^+), \tag{40}$$

where $E_0(A)$ and $E_0(B)$ are the ground-state energies of the atoms A and B, respectively, I_B is the ionization energy of the atom B, and $E_{int}(A-B^+)$ is the energy of interaction of the atom A with the cation B^+. If we allow $\vec{r}_1$ to be in the neighborhood of the other electrons of B^+, it is necessary to take into account that the conditional amplitude will not describe the ground state of B^+. The fact that the system described by Φ is ''distorted'' will correspond to an energy rise ΔE with respect to the ground-state energy. We may therefore write the energy $E^{N-1}(\vec{r}_1\in\Omega_B)$ in general as

$$E^{N-1}(\vec{r}_1\in\Omega_B)\approx E_0(A)+E_0(B)+E_B+E_{int}(A-B^+)+\Delta E(A-B^+;\vec{r}_1). \tag{41}$$

If $R(A-B)$ is large and $\vec{r}_1$ is in the region of the HOMO (i.e., not in the subvalence-core region of B), the effect of the electron redistribution incorporated in the last term is expected to be small.

Contrary to this, the ground state of the cation $(AB)^+$ for large $R(A-B)$ corresponds to the system $A^+—B$ of the neutral atom B interacting with the cation A^+, so that E_0^{N-1} is expressed as

$$E_0^{N-1}\approx E_0(A)+E_0(B)+I_A+E_{int}(A^+-B). \tag{42}$$

Inserting (41) and (42) into (39), we obtain the following expression for $v_{resp}(\vec{r}_1)$:

$$v_{resp}(\vec{r}_1\in\Omega_B)\approx[I_B-I_A]+[E_{int}(A-B^+)-E_{int}(A^+-B)]+\Delta E(A-B^+;\vec{r}_1). \tag{43}$$

Suppose now that the reference electron is in the region Ω_A of the less electronegative atom A, $\vec{r}_1\in\Omega_A$. In this case the conditional amplitude decribes the $(N-1)$-electron system $A^+—B$, disturbed around the reference electron position. If $R(A—B)$ is large and $\vec{r}_1$ is in the region of the HOMO, this system is close to the ground state of the cation $(AB)^+$. As a result, only the corresponding correction term $\Delta E(A^+—B;\vec{r}_1)$ contributes to $v_{resp}(\vec{r}_1)$ in this region

$$v_{resp}(\vec{r}_1\in\Omega_A)=\Delta E(A^+-B;\vec{r}_1). \tag{44}$$

From (43) and (44) we can estimate the buildup Δv_{resp} around the more electronegative atom B

$$\begin{aligned}\Delta v_{resp}&=v_{resp}(\vec{r}_1\in\Omega_B)-v_{resp}(\vec{r}_1\in\Omega_A)\\&=[I_B-I_A]+[E_{int}(A-B^+)-E_{int}(A^+-B)]\\&\quad+[\Delta E(A-B^+;\vec{r}_1\in\Omega_B)\\&\quad-\Delta E(A^+-B;\vec{r}_1\in\Omega_A)].\end{aligned} \tag{45}$$

The leading term of (45) at large bond distances $R(A—B)$ is just the difference of the ionization energies of atoms A and B. Formula (45) demonstrates that the positive buildup $\Delta v_{xc}\approx(I_B-I_A)$ emerges in the response part v_{resp} of v_{xc} or, more precisely, in the v^{N-1} component of v_{resp}. It originates from the difference between the conditional amplitude distribution $|\Phi(s_1,\vec{x}_2,\ldots,\vec{x}_N|\vec{r}_1)|^2$ of $(N-1)$ electrons and the ground-state electron distribution of the cation $(AB)^+$. When $\vec{r}_1\in\Omega_B$, the conditional amplitude distribution corresponds to the system $A—B^+$, while the ground state is the cation A^+-B. Thus, the conditional amplitude, embodying the electron correlation which causes the complete exchange-correlation hole to be located around the reference position, leads to a ''repulsive'' effect on v_{xc} in Ω_B. The KS potential at a point $\vec{r}_1$ in the energetically favorable region, is shifted upwards by a potential barrier of height (I_B-I_A), which emerges from v^{N-1}, to prevent a too strong localization of electrons in that region.

The terms in the second and third square brackets of Eq. (45) provide corrections to the leading term at large $R(A—B)$. The second term represents a correction from the atom-cation interaction, which is different for the pairs $A^+—B$ and $A—B^+$. The third term represents a difference between the energy effects of the redistribution of $(N-1)$ electrons of $A—B^+$ and $A^+—B$ due to the presence of the reference electron position in the outer region of the corresponding charged atom. In other words, the first term brings the main contribution to Δv_{resp} due to the different ionization of A and B, the second one brings a correction due to the different polarization of A and B by a positive charge, and the third one brings a correction due to the different distortions of the cations $A—B^+$ and $A^+—B$ due to the different ''response'' to the proximity of the reference electron position. Since this ''response'' has some relation to the polarizability, and since the polarizability of the less electronegative

atom A is, in general, higher than that of B, both corrections are expected to have a negative sign, opposite to that of the leading term $[I_B - I_A]$.

All the above-mentioned differences tend to decrease with decreasing electronegativity difference of atoms A and B, and turn into zero for the homoatomic molecule A_2 (45), as they should. For A_2 the expression

$$v_{\rm resp}(\vec{r}_1) = \Delta E(A^+ - A; \vec{r}_1), \tag{46}$$

which is an analogue of (44), is valid for the HOMO region and $v_{\rm resp}(\vec{r}_1)$ is expected to be small and to have a flat form in this region. This is true, in particular, for $v_{\rm resp}(\vec{r}_1)$ of the molecule H_2 (see [2] and also the next section).

To sum up, using the partially integrated conditional probability amplitude of the heteroatomic molecule AB, it has been shown that the positive buildup of $v_{\rm xc}$ around the electronegative atom B originates in the v^{N-1} component of the response part of $v_{\rm xc}$. From the asymptotical formulas for $v^{N-1}(\vec{r}_1)$ in different regions an expression for this buildup has been obtained which, in addition to the leading term $(I_B - I_A)$ contains also the polarization and correlation corrections. Examples of the positive buildup of $v_{\rm xc}$ constructed from *ab initio* wave functions for the monohydrides LiH and BH will be presented in the next sections.

IV. CONSTRUCTION OF $v_{\rm xc}$

The scheme of $v_{\rm xc}$ construction used in this paper has been already presented and discussed in [13,18] and here we only mention its main points. The correlated wave functions have been obtained with singly and doubly excited configuration interaction (SDCI) calculations of the ground states at the bond distances $R_e = 1.401$ a.u., $R = 3.0$ a.u., and $R = 5.0$ a.u. for H_2; $R_e = 3.015$ a.u., $R = 5.0$ a.u., and $R = 7.0$ a.u. for LiH; $R_e = 2.330$ a.u., $R = 4.0$ a.u., and $R = 5.0$ a.u. for BH. Calculations have been performed within the direct CI approach by means of the ATMOL package [27].

A basis of contracted Gaussian functions [28] has been used with five s- and two p-type functions for H, seven s-, four p-type functions for Li, seven s- four p- and two d-type functions for B. For H an extra valence polarization d function with the exponent $\alpha = 1.0$ and for Li two such functions with the exponents $\alpha = 0.36$ and $\alpha = 0.15$ have been used. This basis has been already used for the construction of $v_{\rm xc}$ for LiH at the equilibrium bond length [13]. In this paper, in order to better take into account the correlation effects for core electrons, this basis has been augmented for Li and B with two localized polarization p and two d functions of the core size, whose exponents were set equal to those of the second most localized contracted s function of the basis [28]. When compared with the accurate empirical estimates of the Coulomb correlation energies E_c^e at the equilibrium distances [29], the decrease in the correlation energy due to inclusion of core polarization functions amounts to 6% of E_c^e for LiH and 14% for BH, so that the SDCI calculations recover 92% of E_c^e for LiH and 90% for BH. The potential $v_{\rm xc}^{\rm hole}(\vec{r}_i)$ for a given grid $\{\vec{r}_i\}$ has been calculated by integration (21) of the diagonal part $\rho_2(\vec{r}_1, \vec{r}_2)$ of the second-order density matrix, the latter has been calculated from the SDCI wave function by means of a special density-functional extension [2,30] of the *ab initio* ATMOL package.

In the case of the H_2 molecule there is only one occupied KS orbital ϕ_1, so that an accurate $v_{\rm xc}$ is obtained directly from (1) by the replacement of ϕ_1 by $(\rho/2)^{1/2}$ [2]. For XH $v_{\rm xc}(\vec{r})$ and a set of KS orbitals $\{\phi_i(\vec{r})\}$ are obtained from the correlated $\rho(\vec{r})$ with an iterative procedure [10], starting from some initial guess $v_{\rm el}^0$ for $v_{\rm el}$

$$v_{\rm el}^0(\vec{r}) = v_{\rm H}(\vec{r}) + v_{\rm xc}^0(\vec{r}), \tag{47}$$

where $v_{\rm H}$ is the Hartree potential and $v_{\rm xc}^0$ is an approximate exchange-correlation potential of the form

$$v_{\rm xc}^0([\rho]; \vec{r}) = v_{X\alpha}(\rho; \vec{r}) + 2\epsilon_x^B(\rho, |\nabla\rho|; \vec{r}) + 2\epsilon_c^{\rm VWN}(\rho; \vec{r}), \tag{48}$$

both potentials being calculated with the correlated density ρ. In (48) $v_{X\alpha}$ is the exchange-correlation $X\alpha$ potential [31], ϵ_x^B is the exchange energy density gradient correction of Becke [32], and $\epsilon_c^{\rm VWN}$ is the local-density approximation (LDA) of Vosko, Wilk, and Nusair [33] for the correlation energy density. The potential (47) has a proper long-range Coulombic asymptotics $v_{\rm el}^0 \to (N-1)/|r|$. For the equilibrium bond length the parameter $\alpha_{\rm eq}$ of $v_{X\alpha}$ is chosen from the following fitting condition:

$$[-\tfrac{1}{2}\nabla^2 + v_{\rm ext}(\vec{r}) + v_{\rm el}^0(\vec{r})]\phi_N(\vec{r}) = -I_p\phi_N(\vec{r}), \tag{49}$$

where ϕ_N is the HOMO and I_p is the experimental ionization energy of the molecule. For larger distances $R(X$—H) the parameter α is varied starting from $\alpha_{\rm eq}$ and, finally, the value α is used, which provides the quickest convergence of the iterative procedure.

At mth iteration KS equations (1) are solved with the potential $v_{\rm el}^m$

$$v_{\rm el}^m(\vec{r}) = f_m(\vec{r}) v_{\rm el}^{m-1}(\vec{r}) \tag{50}$$

calculated from $v_{\rm el}^{m-1}$ of the previous iteration with the correction factor f_m, the latter being defined with the density ρ^{m-1} from the $(m-1)$th iteration and the *ab initio* target density ρ

$$f_m(\vec{r}) = \frac{\rho^{m-1}(\vec{r}) + a}{\rho(\vec{r}) + a} \tag{51}$$

with the parameter $a = 0.5$, which smooths out the effect of the remote exponential density tails on the procedure. Then, ρ^{m-1} in (51) is replaced with ρ^m obtained at mth iteration and this procedure continues unless further iterations cease lowering the difference $|\rho^m(\vec{r}) - \rho(\vec{r})|$ in the region of nonvanishing densities. Finally, $v_{\rm xc}(\vec{r})$ is obtained by subtracting $v_{\rm H}(\vec{r})$ from the resulting potential (50). Construction of $v_{\rm xc}$ has been performed in the same basis of MO's as the SDCI calculations by means of the above-mentioned density-functional extension [2,30] of the ATMOL package. Matrix elements of $v_{\rm el}^m$ in this basis have been calculated using a numerical integration with grids according to Ref. [34].

After 45–50 iterations the procedure has reached its saturation state and further several hundred iterations make changes only within 0.001–0.003 a.u. for the obtained values of ϵ_N and the KS kinetic energy T_s and produce basically the same KS orbitals $\{\phi_i(\vec{r})\}$. However, after 200–250 iterations

TABLE I. Kohn–Sham energy characteristics (a.u.) for LiH at various bond distances R(Li—H) (a.u.).

R(Li—H)	3.015	5.0	7.0
ϵ_{HOMO}	−0.284	−0.238	−0.206
$-I_p$	−0.283		−0.198
T_s	8.001	7.823	7.826
T^{HF}	7.993	7.787	7.747
T^{CI}	8.058	7.880	7.876
T_c	0.057	0.057	0.050
$T_{c,\mathrm{HF}}$	0.065	0.093	0.129

TABLE II. Kohn-Sham energy characteristics (a.u.) for BH at various bond distances R(B—H) (a.u.).

R(B—H)	2.33	4.0	5.0
ϵ_{HOMO}	−0.359	−0.346	−0.334
$-I_p$	−0.359		−0.305
T_s	25.153	24.883	24.893
T^{HF}	25.119	24.793	24.757
T^{CI}	25.252	24.980	24.985
T_c	0.099	0.097	0.092
$T_{c,\mathrm{HF}}$	0.133	0.187	0.228

(depending on the type of system and the bond distance) visible and (presumably) artificial long-range oscillations are developed in v_{xc}, which do not alter the above-mentioned KS characteristics but disturb the form of v_{xc}. For larger bond distances these oscillations arise at earlier iterations than for R_e.

The development of the (spurious) long-range oscillations of v_{xc} after several hundred iterations seems to be an artifact of the finite basis set used in the molecular calculations, since no such effect appears in the numerical atomic calculations with the procedure (47),(50),(51) [10]. The effect of the finite basis restriction on the constructed v_{xc} has been mentioned in [35]. The possibility of these oscillations follows from the fact that, in principle, an oscillating function can be added to v_{xc}, such that its addition does not change matrix elements of v_{xc} in a given finite basis. Though not disturbing the integral characteristics, the development of these oscillations can be recognized by the increasing of the maximal local relative difference

$$\Delta\rho_m^{\max}=\max_{\vec{r}\in\Omega}\frac{|\rho^m(\vec{r})-\rho(\vec{r})|}{\rho(\vec{r})} \tag{52}$$

(Ω is the region of nonvanishing densities) between the target density ρ and the density ρ^m starting from a certain (m_t+1)th iteration. In our present calculations, in order to prevent the development of the spurious oscillations, we terminate the iterative procedure at the m_tth iteration, at which the difference (52) attains its minimum for $\rho>0.1$ a.u. The corresponding $\Delta\rho_{m_t}^{\max}$ values are within 0.1–0.2%.

The potential $v_{c,\mathrm{kin}}(\vec{r})$ has been calculated from the SDCI first-order density matrix $\rho(\vec{r}',\vec{r})$ and the KS density matrix $\rho(\vec{r}',\vec{r})=\Sigma_{i=1}^{N}\phi_i^*(\vec{r}')\phi_i(\vec{r})$ obtained with the iterative procedure discussed above. Finally, $v_{\mathrm{resp}}(\vec{r})$ has been obtained by subtraction of $v_{c,\mathrm{kin}}(\vec{r})$ and $v_{\mathrm{xc}}^{\mathrm{hole}}(\vec{r})$ from the constructed $v_{\mathrm{xc}}(\vec{r})$. The results of the scheme presented in this section will be discussed in the next sections.

V. KOHN-SHAM ENERGY CHARACTERISTICS

Tables I and II present various energy characteristics for the KS orbitals $\{\phi_i(\vec{r})\}$ of the LiH and BH for three different bond distances $R(X$—H). The first is the HOMO energy ϵ_N. According to [36–39] an accurate HOMO energy ϵ_N is equal to minus the ionization potential of the system I_p. In the dissociation limit the ionization potential of XH approaches that of the less electronegative atom X, so that ϵ_N should follow the same trend. One can see from Tables I and II that ϵ_N values obtained for XH at the equilibrium distance $R_e(X$—H) are indeed very close to the experimental $-I_p$ values (the latter quantities are placed in Tables I and II just below the former ones). For both systems ϵ_N decreases (in absolute magnitude) with increasing R and for the largest R value it is not far from $-I_p$ value of the X atom (the latter quantities are also placed just below the former ones).

Tables I and II also present the kinetic energy of the KS system T_s

$$T_s=-\frac{1}{2}\sum_{i=1}^{N}\int\phi_i^*(\vec{r})\nabla^2\phi_i(\vec{r})d\vec{r} \tag{53}$$

and the kinetic part of the exchange-correlation energy T_c

$$T_c=T^{\mathrm{CI}}-T_s=\int\rho(\vec{r})v_{c,\mathrm{kin}}(\vec{r})d\vec{r}. \tag{54}$$

T_s is compared with the CI T^{CI} and the Hartree-Fock T^{HF} kinetic energies, while T_c is compared with the kinetic part $T_{c,\mathrm{HF}}$ of the conventional correlation energy

$$T_{c,\mathrm{HF}}=T^{\mathrm{CI}}-T^{\mathrm{HF}}. \tag{55}$$

In Table III the same kinetic characteristics are presented for the H_2 molecule.

In all cases the T_s value is placed in between the corresponding T^{HF} and T^{CI} ones

$$T^{\mathrm{HF}}<T_s<T^{\mathrm{CI}}. \tag{56}$$

The right-hand inequality of (56) follows from the fact that both T_s and T^{CI} correspond to the same correlated density ρ and T_s, by its definition [40], delivers the minimal kinetic energy for this density. The left-hand inequality reflects the difference between the Hartree-Fock and correlated densities. It is well known that the correlated density is more

TABLE III. Kinetic energy characteristics (a.u.) for H_2 at various bond distances R(H—H) (a.u.).

R(H—H)	1.401	3.0	5.0
T_s	1.140	0.831	0.955
T^{HF}	1.125	0.713	0.650
T^{CI}	1.172	0.872	0.977
T_c	0.032	0.041	0.022
$T_{c,\mathrm{HF}}$	0.047	0.159	0.327

contracted around the nuclei than the Hartree-Fock one, which is extremely so in poor Hartree-Fock cases like dissociating H_2 [2,20]. Due to this contraction effect of correlation, the minimal energy T_s is still higher than T^{HF}.

For H_2 and BH T^{CI} value at the intermediate bond distance is lower than those at the larger and equilibrium distances, while for LiH T^{CI} values at $R=5.0$ and 7.0 a.u. are close to each other, both being appreciably lower than that at $R_e=3.015$ a.u. It is an anticipated trend since, according to the virial theorem formula [41]

$$T=-E_0^N-R\,\frac{dE_0^N}{dR}, \tag{57}$$

the exact kinetic energy T has a negative contribution from the Hellmann-Feynman forces at larger distances, which vanishes at both $R=R_e$ and $R\to\infty$, so that T as a function of R passes through a minimum at $R>R_e$. For the restricted CI the virial theorem holds only approximately, still T^{CI} exhibits a similar behavior. The virial theorem is accomplished through a lowering of the gradient of the wave function (more precisely, its z component in the bond axis direction) which entails a lowering of the corresponding component $T_{\|}$ [42–44]. As a consequence, the z component of the density gradient also decreases and T_s has a similar behavior as T^{CI}: for all three systems the T_s value at intermediate R is lower than those at larger and equilibrium R. For T^{HF} Eq. (57) holds true if E_0^N is replaced with the Hartree-Fock total energy E_{HF}. However, in this case a negative contribution of the second term is overcompensated with the gradual decrease of E_{HF} at larger distances, so that for the distances considered T^{HF} monotonically decreases with the increasing R.

The comparative features of T_s, T^{HF}, and T^{CI} discussed above determine those of their differences T_c and $T_{c,\mathrm{HF}}$. Because of Eq. (56), both T_c and $T_{c,\mathrm{HF}}$ are always positive and because of the left-side inequality of (56) T_c is consistently lower than $T_{c,\mathrm{HF}}$. The molecular dissociation has a strikingly different effect on $T_{c,\mathrm{HF}}$ and T_c. Due to the near-degeneracy effect (which is not taken into account in the restricted Hartree-Fock method), the left-right correlation is strengthened at larger bond distances, which causes an increase of $T_{c,\mathrm{HF}}$. Contrary to this, in the dissociation limit T_c approaches to the sum of the T_c contributions of the atomic fragments, which is lower than the molecular T_c value at R_e.

In particular, for the one-electron H atom $T_c=0$, since in this case the KS system coincides with the exact one, so that for the H_2 molecule T_c should approach zero in the dissociation limit and for XH T_c should approach the corresponding value for the individual atom X. This zero asymptotics for H_2 can be easily derived, if we employ the fact that in this limit the H_2 molecule is described properly with the Heitler-London wave function $\Psi^{\mathrm{HL}}(\vec{x_1},\vec{x_2})$

$$\Psi^{\mathrm{HL}}(\vec{x_1},\vec{x_2})=\frac{a^*(\vec{r}_1)b(\vec{r}_2)+a^*(\vec{r}_2)b(\vec{r}_1)}{2(1+S_{ab}^2)^{1/2}}\times[\alpha(s_1)\beta(s_2)-\alpha(s_2)\beta(s_1)], \tag{58}$$

where $a(\vec{r})$ and $b(\vec{r})$ are the $1s$-type atomic orbitals located on the H atoms A and B, $\alpha(i)$ and $\beta(i)$ are the one-electron spin functions and S_{ab} is the overlap integral

$$S_{ab}=\int a^*(\vec{r})b(\vec{r})d\vec{r}. \tag{59}$$

A convenient feature of the Kohn-Sham theory is that even in the dissociation limit the Kohn-Sham system of H_2 is properly described with the one-determinantal wave function $\Psi_s(\vec{x_1},\vec{x_2})$ formed from the $1s$ orbitals $a(\vec{r})$ and $b(\vec{r})$

$$\Psi_s(\vec{x_1},\vec{x_2})=\frac{[a^*(\vec{r}_1)+b^*(\vec{r}_1)][a(\vec{r}_2)+b(\vec{r}_2)]}{2\sqrt{2}(1+S_{ab})}\times[\alpha(s_1)\beta(s_2)-\alpha(s_2)\beta(s_1)], \tag{60}$$

since $\Psi_s(\vec{x_1},\vec{x_2})$ still generates the ground-state density $\rho(\vec{r})$ in this limit. Subtracting the kinetic energy obtained with $\Psi_s(\vec{x_1},\vec{x_2})$ from that obtained with $\Psi^{\mathrm{HL}}(\vec{x_1},\vec{x_2})$, one can derive an asymptotic expression for T_c

$$T_c=\langle\Psi^{\mathrm{HL}}|\hat{T}|\Psi^{\mathrm{HL}}\rangle-\langle\Psi_s|\hat{T}|\Psi_s\rangle=\frac{2(T_aS_{ab}-T_{ab})(1-S_{ab})}{(1+S_{ab})(1+S_{ab}^2)}, \tag{61}$$

where T_a and T_{ab} are the kinetic integrals

$$T_a=-\frac{1}{2}\int a^*(\vec{r})\nabla^2a(\vec{r})d\vec{r}, \tag{62}$$

$$T_{ab}=-\frac{1}{2}\int a^*(\vec{r})\nabla^2b(\vec{r})d\vec{r}. \tag{63}$$

The difference between total energies obtained with $\Psi^{\mathrm{HL}}(\vec{x_1},\vec{x_2})$ and $\Psi_s(\vec{x_1},\vec{x_2})$, the correlation energy E_c, approaches with increasing H—H distance its exact finite limiting value -0.3125 a.u. [31]. On the other hand T_c the difference (61) between the corresponding kinetic energies decreases with the decreasing S_{ab} and T_{ab} at longer bond distances and it becomes zero in the infinite separation limit

$$T_c\to 0, \quad R(\mathrm{H—H})\to\infty. \tag{64}$$

The results of the calculations presented in Tables I–III agree with the asymptotics derived theoretically. For H_2 the T_c value calculated at $R(\mathrm{H—H})=5.0$ a.u. is nearly twice as small as the corresponding value at $R(\mathrm{H—H})=3.0$ a.u. (See Table III). In a similar way, for XH the T_c values calculated at the largest distance considered are the least ones (See Tables I and II) and they are rather close to the T_c values 0.038 a.u. and 0.095 a.u. obtained for the atoms Li and B, respectively, in [12]. As a consequence, in all cases the ratio $T_c/T_{c,\mathrm{HF}}$ gradually decreases with increasing bond distance. The local behavior of the potential $v_{c,\mathrm{kin}}$ which determines T_c via the integral (54), as well as the form of other potentials will be discussed in the next section.

VI. v_{xc} AND ITS COMPONENTS

Figures 2–4 compare the molecular Kohn-Sham exchange-correlation potentials v_{xc} and the potentials of the exchange-correlation hole $v_{\mathrm{xc}}^{\mathrm{hole}}$ constructed for H_2 and XH

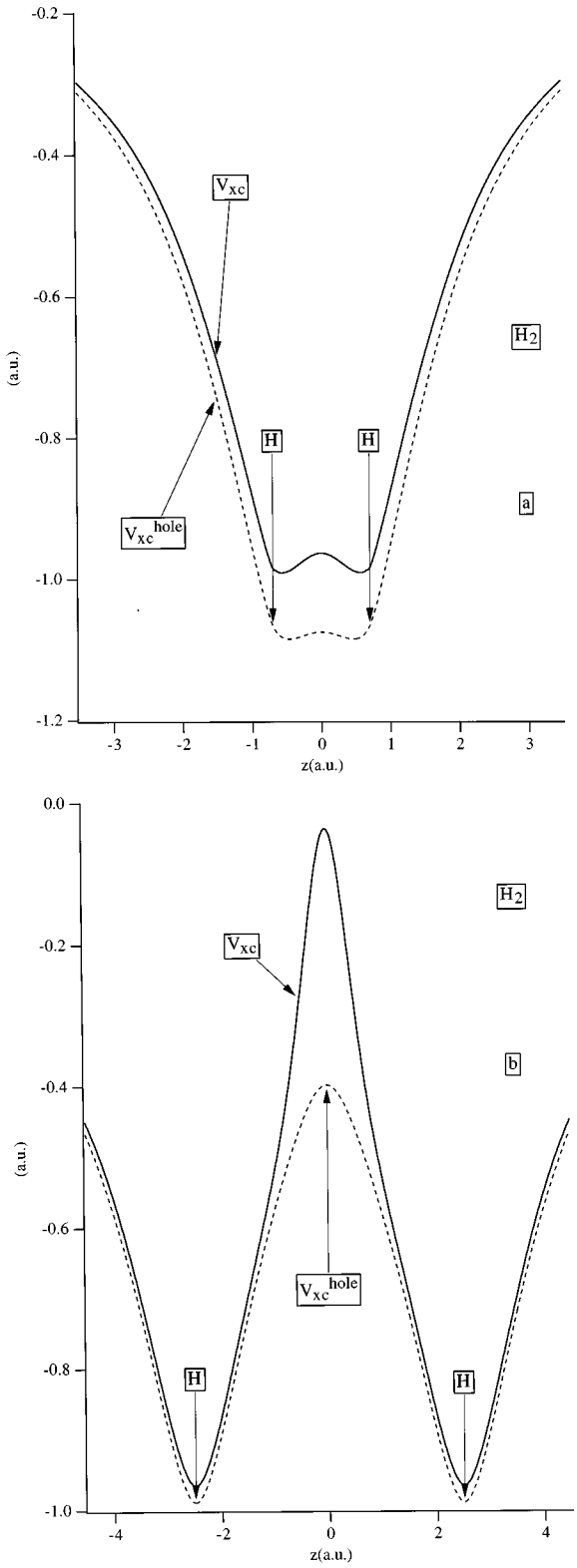

FIG. 2. Kohn-Sham exchange-correlation potential and the potential of the exchange-correlation hole for H_2. (a) $R_e=1.401$ a.u. and (b) $R=5.0$ a.u.

(X=Li, B) for the equilibrium R_e and larger bond distances. The potentials are plotted along the bond axis as functions of the distance z from the bond midpoint. In all cases both $v_{\rm xc}$ and $v_{\rm xc}^{\rm hole}$ are negative functions, with $v_{\rm xc}$ being consistently less attractive than the corresponding $v_{\rm xc}^{\rm hole}$. This is quite understandable, since $v_{\rm xc}^{\rm hole}$ represents the main correlation effect of reduction of the electron-electron repulsion due to the formation of the exchange-correlation hole. According to Eq. (35), $v_{\rm xc}$ is formed by the addition of $v_{c,\rm kin}$ and $v_{\rm resp}$ to $v_{\rm xc}^{\rm hole}$, and the former potentials represent the repulsive effect of the ''perturbation'' of the $(N-1)$-electron system by the reference electron and the repulsive kinetic effect, respectively.

As expected, the molecular dissociation has relatively little effect on the form of $v_{\rm xc}$ and $v_{\rm xc}^{\rm hole}$ in the inner region of atom X (See Figs. 3, 4). Both $v_{\rm xc}$ and $v_{\rm xc}^{\rm hole}$ in this region have a deep well around the nucleus X, which represents the self-interaction part of the exchange potential of the $1s$ electron. At positions r within the $1s$ shell the exchange hole surrounding r is very close to minus the $1s$ density. Between the core and valence regions $v_{\rm xc}$ exhibits characteristic local maxima (intershell peaks). For BH one can see these peaks on both inner (with respect to the bond) and outer sides of the B atom and dissociation makes the outer-side peak more pronounced (See Fig. 4).

$v_{\rm xc}$ for LiH exhibits a similar peak only on the inner side of the Li atom (See Fig. 3), while on the outer side the intershell region is characterized only by a change of the slope of $v_{\rm xc}$. Dissociation makes this ''peak'' smaller, so that at large distance $R=7.0$ a.u. $v_{\rm xc}$ in this region looks more like $v_{\rm xc}$ of the individual Li atom, which virtually lacks the intershell peak (See Fig. 2 of Ref. [12]). Unlike $v_{\rm xc}$, $v_{\rm xc}^{\rm hole}$ is a more smooth potential: for both XH systems $v_{\rm xc}^{\rm hole}$ is a monotonical function of z in the intershell regions for larger R, while for R_e it exhibits much more shallow local maxima, which are displaced towards the bond midpoint.

The molecular dissociation manifests itself in the formation of a characteristic peak of $v_{\rm xc}$ near (or at) the bond midpoint $z=0$. The H_2 molecule provides an extreme example of such a peak (See Fig. 2). In this case $v_{\rm xc}$ already has a small bond midpoint peak for $R_e=1.401$ a.u. However, it increases dramatically with increasing bond length, the corresponding maximum of $v_{\rm xc}$ is close to zero. The peak grows both in absolute value and with respect to $v_{\rm xc}^{\rm hole}$, so that one can consider a formation of the bond midpoint peak on top of $v_{\rm xc}^{\rm hole}$.

In the case of XH dissociation also creates, though visually less spectacular, a rather shallow peak of $v_{\rm xc}$ in the bonding region. It is displaced from $z=0$ towards the H nucleus: for LiH at $R=7.0$ a.u. $v_{\rm xc}$ reaches a local maximum at $z=0.70$ a.u., while for BH at $R=5.0$ a.u. this maximum is at $z=0.59$ a.u.. Unlike for the H_2 molecule, for both XH molecules the position of the peak does not coincide with the corresponding local minimum of the density ρ for the interatomic part of the bond axis, the latter being placed at $z=-0.05$ a.u. for LiH and at $z=0.41$ a.u. for BH.

Formation of the peak is accompanied with formation of a local well of $v_{\rm xc}$ just beyond the inner-side intershell peak. The corresponding minimum of $v_{\rm xc}$ is placed at $z=-0.86$ a.u. for LiH at $R=7.0$ a.u. and at $z=-1.16$ a.u. for BH at $R=5.0$ a.u. and $v_{\rm xc}$ nearly touches $v_{\rm xc}^{\rm hole}$ at these points. One can see from Figs. 3(b) and 4(b) that the above-mentioned structure of $v_{\rm xc}$ in the bonding region is built up on top of $v_{\rm xc}^{\rm hole}$, the latter potential being a rather smooth function in this region. From this it follows that other parts of $v_{\rm xc}$, namely, $v_{c,\rm kin}$ and $v_{\rm resp}$ are responsible for this structure and we shall proceed with the analysis of these parts.

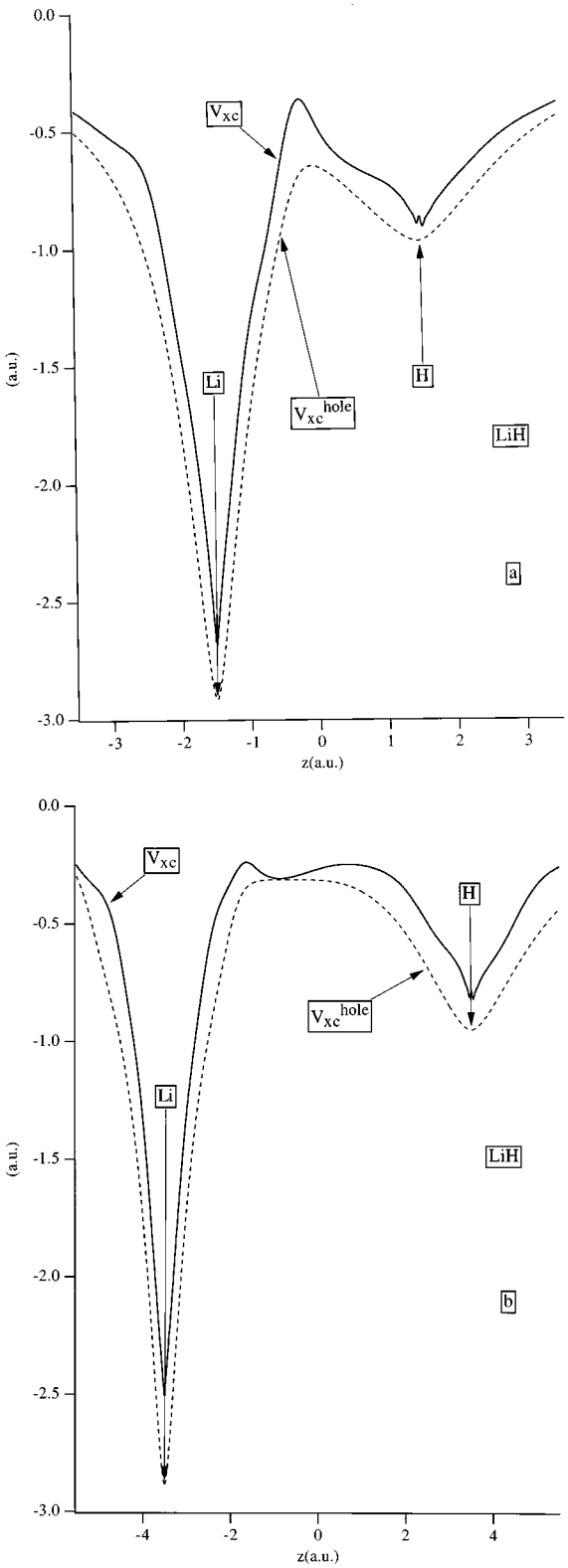

FIG. 3. Kohn-Sham exchange-correlation potential and the potential of the exchange-correlation hole for LiH. (a) $R_e=3.015$ a.u. and (b) $R=7.0$ a.u.

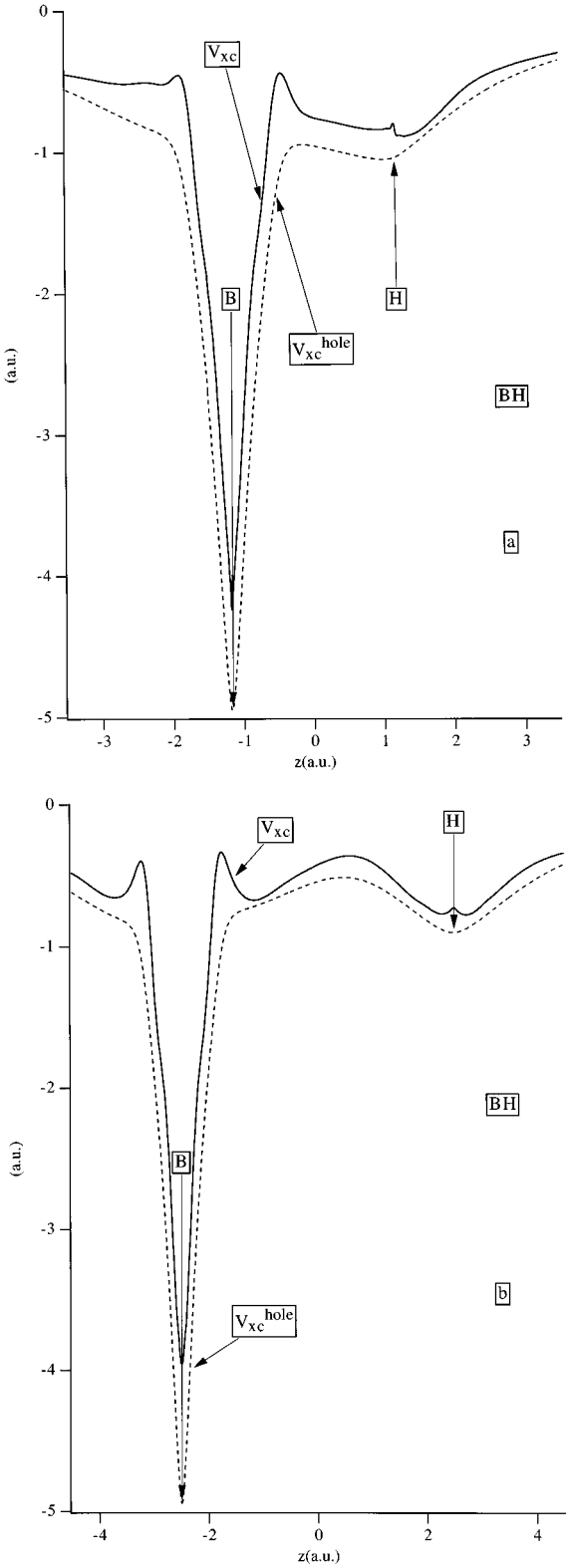

FIG. 4. Kohn-Sham exchange-correlation potential and the potential of the exchange-correlation hole for BH. (a) $R_e=2.33$ a.u. and (b) $R=5.0$ a.u.

Figure 5 compares the potentials $v_{c,\mathrm{kin}}$ obtained for H_2, LiH, and BH at the same elongated bond distance $R=5.0$ a.u. [note that for the two-electron system H_2 $v_{c,\mathrm{kin}}$ reduces to the potential v_{kin} of Eq. (22)]. In all cases $v_{c,\mathrm{kin}}$ exhibits a positive peak in the bonding region, though for XH these peaks are much smaller than that for H_2. The peak grows higher with increasing bond length. One can see this from Fig. 6 where $v_{c,\mathrm{kin}}$ constructed at two different bond distances R are compared in the region of the bond peak for H_2 and LiH.

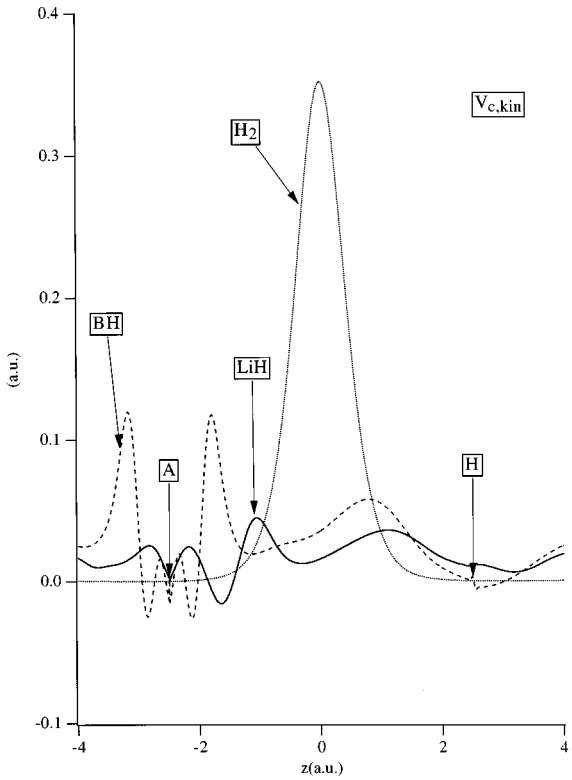

FIG. 5. Comparison of the potentials $v_{c,\mathrm{kin}}$ for H_2, LiH, and BH at $R=5.0$ a.u.

The behavior of $v_{c,\mathrm{kin}}$ in the bonding region reflects the effect of the left-right correlation of electrons of a single bond X—H on the conditional amplitude $\Phi(s_1, \vec{x}_2,\ldots,\vec{x}_N|\vec{r}_1)$. According to its definition (28), the relatively small $v_{c,\mathrm{kin}}(\vec{r}_1)$ is a difference of two bigger potentials $v_{\mathrm{kin}}(\vec{r}_1)$ and $v_{s,\mathrm{kin}}(\vec{r}_1)$. In its turn, the latter difference is determined according to Eqs. (22), (25) by the integrated difference of the conditional amplitude gradients $|\nabla_1\Phi(s_1,\vec{x}_2,\ldots,\vec{x}_N|\vec{r}_1)|^2$ and $|\nabla_1\Phi_s(s_1,\vec{x}_2,\ldots,\vec{x}_N|\vec{r}_1)|^2$ or, in other words, by the relative sensitivity of the exchange-correlation and exchange (Fermi) holes in the distribution of other electrons to the displacement of the reference electron from $\vec{r}_1$. If $\vec{r}_1$ is in the bonding region and the reference electron is displaced from $\vec{r}_1$ towards a certain atom, another electron of the single bond gets an increase of its probability distribution on the other atom due to the left-right Coulomb correlation. This causes a change of the exchange-correlation hole associated with $\Phi(s_1,\vec{x}_2,\ldots,\vec{x}_N|\vec{r}_1)$ and produces a certain positive value of the amplitude gradient $|\nabla_1\Phi(s_1,\vec{x}_2,\ldots,\vec{x}_N|\vec{r}_1)|^2$. Since there is no analogous exchange effect, the resulting $v_{c,\mathrm{kin}}$ is definitely positive in this region. For the homoatomic H_2 molecule $v_{c,\mathrm{kin}}$ attains a maximum just at the bond midpoint $z=0$, while for XH the corresponding maxima are displaced towards the H atom.

The left-right correlation is strengthened at larger bond distances by the strong near-degeneracy effect. As a consequence, the bond peak of $v_{c,\mathrm{kin}}$ grows higher and Fig. 6 clearly illustrates this trend. In the case of H_2 $v_{c,\mathrm{kin}}$ provides a dominating contribution to the bond peak of v_{xc} at large distances R. For XH $v_{c,\mathrm{kin}}$ also makes a substantial contribution to the bond peak of v_{xc}, though in this case the corresponding contribution of the response potential v_{resp} is somewhat larger (see the discussion below). In spite of the development of a high peak, $v_{c,\mathrm{kin}}$ yields, after the multiplication by ρ and integration (Eq. 54), a lower value of the correlation kinetic energy T_c for R(H—H)$=5.0$ a.u. than that

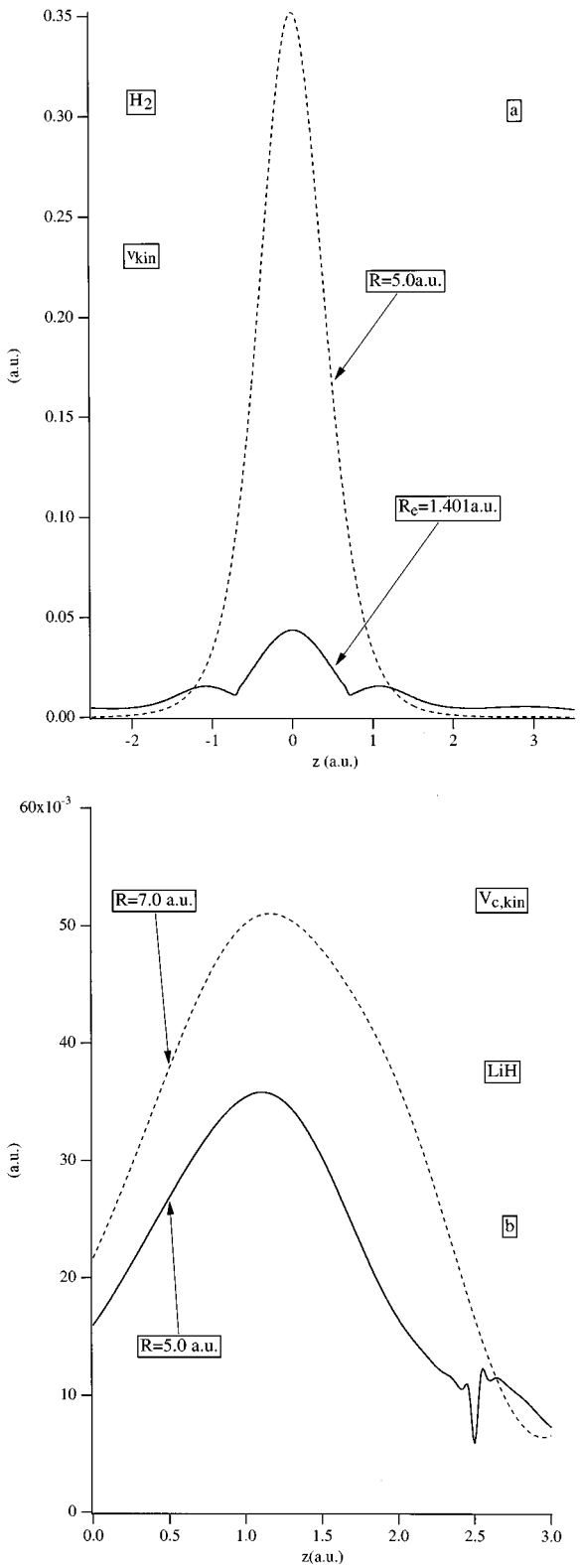

FIG. 6. Comparison of the potentials $v_{c,\mathrm{kin}}$ constructed at various bond distances. (a) H_2, $R_e=1.401$ a.u. and $R=5.0$ a.u. and (b) LiH, $R=5.0$ a.u. and $R=7.0$ a.u.

for R_e (See Table III). An evident reason for this is that the peak arises in the bond midpoint region, which is the region of a low density ρ at large R(H—H). The same trend, though not so spectacularly expressed, holds true also for the monohydrides XH.

While for all systems $v_{c,\mathrm{kin}}$ vanishes in the region of the H atoms, it displays an oscillating behavior in the region of the X atoms of XH (See Fig. 5). The oscillations tend to be more contracted for the heavier atom B, the most visible feature being the positive peaks in the intershell regions. This oscillating behavior reflects different relative sensitivity of the exchange-correlation and Fermi holes associated with $\Phi(s_1,\vec{x}_2,\ldots,\vec{x}_N|\vec{r}_1)$ and $\Phi_s(s_1,\vec{x}_2,\ldots,\vec{x}_N|\vec{r}_1)$ to the displacement of the reference electron from $\vec{r}_1$ for different positions $\vec{r}_1$ in this region. The interpretation of this complicated behavior will be given elsewhere. We have no explanation for the sharp dip at the nuclei, which is possibly caused by the unphysical Gaussian shape of our CI density at the nucleus.

In Figs. 7, 8 the response potentials v_{resp} are plotted, which have been obtained by subtraction of $v_{\mathrm{xc}}^{\mathrm{hole}}$ and $v_{c,\mathrm{kin}}$ from v_{xc}. To make the interpretation of its form more clear, in Fig. 7 v_{resp} is compared with the model potential $v_{\mathrm{resp}}^{\mathrm{mod}}$ [45]

$$v_{\mathrm{resp}}^{\mathrm{mod}}(\vec{r})=\sum_{i=1}^{N} w_i \frac{|\phi_i(\vec{r})|^2}{\rho(\vec{r})}, \tag{65}$$

the latter being the statistical average of the orbital contributions w_i

$$w_i=K\sqrt{\mu-\epsilon_i}. \tag{66}$$

The potential (65,66) with $K=0.38$ models the response part of the Krieger-Li-Iafrate (KLI) [46] approximation v_x^{KLI} to the exchange potential v_x^{OPM} of the optimized potential model (OPM) [47–49]

$$v_x^{\mathrm{KLI}}(\vec{r})=v_x^{\mathrm{hole}}(\vec{r})+\sum_{i=1}^{N} w_i \frac{|\phi_i(\vec{r})|^2}{\rho(\vec{r})}. \tag{67}$$

The parameters w_i were defined within the KLI approximation in a self-consistent way as the difference between the expectation values of the potential (67) and the Hartree-Fock exchange operator v_{xi} for the orbital ϕ_i

$$w_i=\int |\phi_i(\vec{r})|^2[v_x^{\mathrm{KLI}}(\vec{r})-v_{xi}(\vec{r})]d\vec{r}, \tag{68}$$

$$v_{xi}(\vec{r}_1)=-\frac{1}{\phi_i(\vec{r}_1)}\sum_{j=1}^{N}\phi_j(\vec{r}_1)\int\frac{\phi_i(\vec{r}_2)\phi_j(\vec{r}_2)}{|\vec{r}_1-\vec{r}_2|}d\vec{r}_2, \tag{69}$$

and $v_x^{\mathrm{hole}}(\vec{r})$ in (67) is the potential of the Fermi hole, the exchange-only analogue of $v_{\mathrm{xc}}^{\mathrm{hole}}(\vec{r})$

$$v_x^{\mathrm{hole}}(\vec{r})=\sum_{i=1}^{N} v_{xi}(\vec{r})\frac{|\phi_i(\vec{r})|^2}{\rho(\vec{r})}. \tag{70}$$

The model (65,66) has the same orbital structure as the KLI construction and it satisfies the same condition [46] of zero contribution of the HOMO to the numerator of (65)

$$w_N=0. \tag{71}$$

As was shown in [45], for atomic systems $v_{\mathrm{resp}}^{\mathrm{mod}}$ reproduces the characteristic stepped form of the response part of v_x^{OPM} and its KLI approximation.

Due to its construction (65), $v_{\mathrm{resp}}^{\mathrm{mod}}$ has a clear stepped form that helps to visualize the regions of various MO's (See Fig. 7). The region of the core $1s$ electrons of atom X is characterized by a high plateau of $v_{\mathrm{resp}}^{\mathrm{mod}}$, while beyond this region $v_{\mathrm{resp}}^{\mathrm{mod}}$ has a steep descent to low values and it vanishes in the region of the HOMO around the H atom. This short-range behavior of $v_{\mathrm{resp}}^{\mathrm{mod}}$ follows from the KLI condition (71), so that all KLI-like potentials of the form (65) with (71) are expected to vanish in a similar way in the region of the HOMO. $v_{\mathrm{resp}}^{\mathrm{mod}}$ displays the above-mentioned features at both equilibrium and larger distances [Compare Figs. 7(a) and 7(c)]. When comparing the form of the potential for LiH and BH, one can note in the latter case an additional ''shoulder'' of $v_{\mathrm{resp}}^{\mathrm{mod}}$ in between the core and the HOMO regions. This can be attributed to the occupied nonbonding MO of BH formed, mainly, from the $2s$ orbital of the B atom.

In the region of atom X $v_{\mathrm{resp}}^{\mathrm{mod}}$ agrees qualitatively with the constructed v_{resp}. Though far from perfect, the one-step structure can be recognized for v_{resp} with higher values for the core electrons and lower values for other electrons. v_{resp} and $v_{\mathrm{resp}}^{\mathrm{mod}}$ display a steep descent to low values in the same regions, which is especially true for larger bond distances [See Figs. 7(a) and 7(b)]. The average height of v_{resp} in the core region appears to be somewhat lower than the step height of $v_{\mathrm{resp}}^{\mathrm{mod}}$ calculated with $K=0.38$, the corresponding relative difference is larger for LiH.

The step pattern of v_{resp} in the region of atom X is disturbed, mainly, by the cusps and wiggles near the nuclei. One of the possible reasons for these features can be the inclusion of the correlation effects. Other reasons can be the deficiency of the Gaussian basis set representation of the CI density at the nucleus and the performance of the numerical procedure of v_{xc} construction. Because of the singularity of the derivative of ρ at nuclei, it appears to be somewhat difficult, in general, to achieve high accuracy close to nuclei, which of course is virtually impossible with Gaussian orbital based densities [4,11,13,14].

Unlike in the core regions, v_{resp} and $v_{\mathrm{resp}}^{\mathrm{mod}}$ have a very different behavior in the HOMO region. As was discussed above, $v_{\mathrm{resp}}^{\mathrm{mod}}$ vanishes in this region. Contrary to this, v_{resp} passes through a local minimum and then develops a positive buildup around the H atom, which is a more electronegative atom for both LiH and BH. One can draw the conclusion that the constructed v_{resp} possesses a true feature, which has been established for v_{resp} of the heteroatomic molecule in Sec. III, namely, the positive buildup of v_{resp} around the more electronegative atom. Though the theoretical results of Sec. III have been obtained for the asymptotical case of large distances $R(A—B)$, the same qualitative picture holds true for both larger and equilibrium distances [compare Figs. 7(a) and 7(c)].

Based on the present analysis, one can expect that the KLI potential (67) lacks the positive buildup around the more electronegative atom. Indeed, the v_x^{hole} term of (67) has a similar smooth form as $v_{\mathrm{xc}}^{\mathrm{hole}}$ presented here, while the sec-

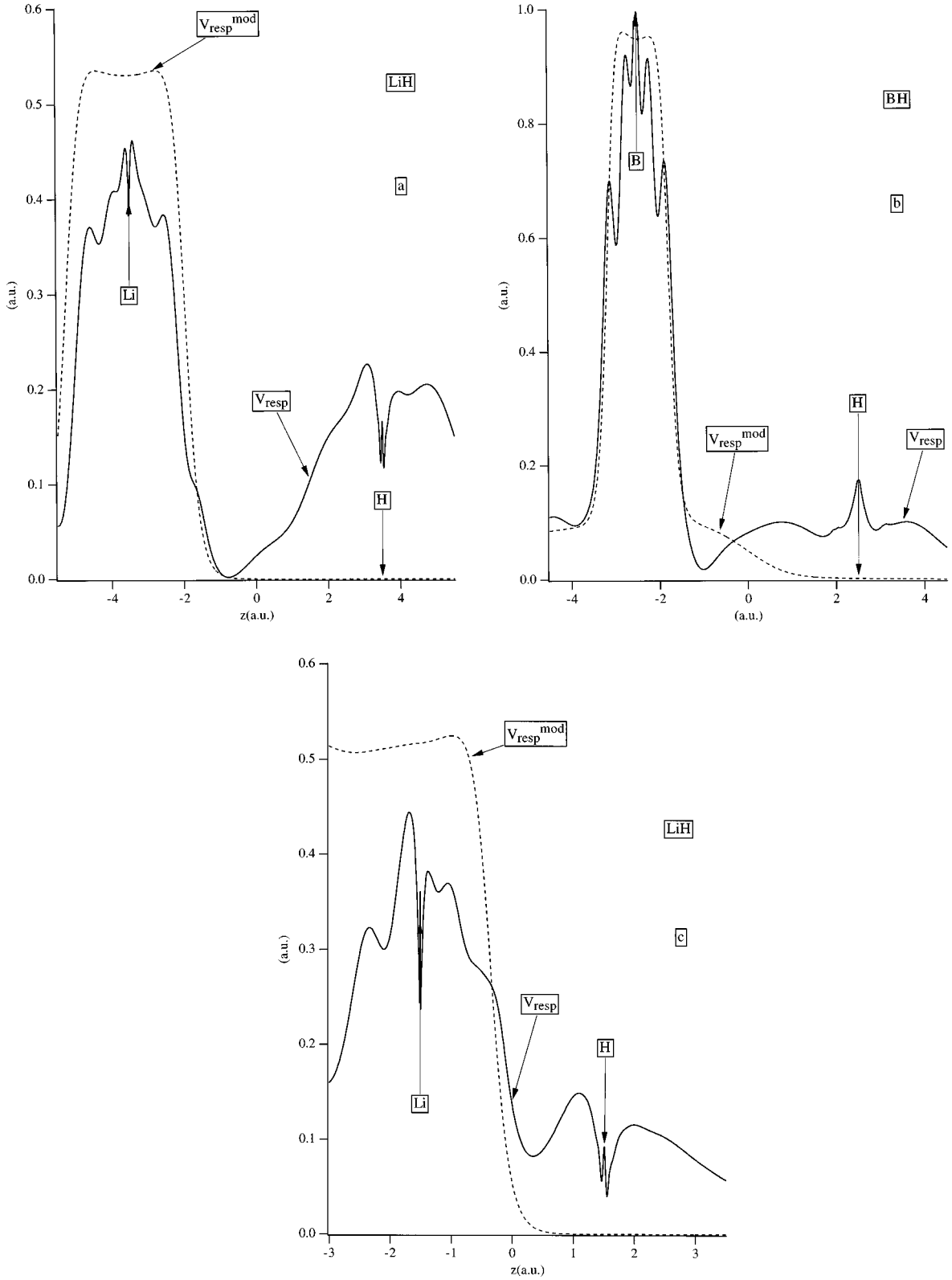

FIG. 7. Comparison of the potentials v_{resp} and $v_{\mathrm{resp}}^{\mathrm{mod}}$ (a) LiH, $R=7.0$ a.u. and (b) BH, $R=5.0$ a.u. and (c) LiH, $R_e=3.015$ a.u.

ond term of (67) has the same structure as $v_{\mathrm{resp}}^{\mathrm{mod}}$ and the latter potential demonstrates the absence of the above-mentioned feature. When comparing v_{xc} and v_x^{KLI}, the positive build-up appears as a correlation effect for the heteroatomic molecules, which is present in the exchange-correlation potential v_{xc} and is absent in the exchange-only potential v_x^{KLI}. Also the bond midpoint peak due to $v_{c,\mathrm{kin}}$ would be absent in v_x^{KLI}.

The inclusion of the positive buildup is essential in order to provide the proper energies ϵ_N of the HOMO. Because of its absence, the HOMO energies obtained for LiH and BH with the combined potential

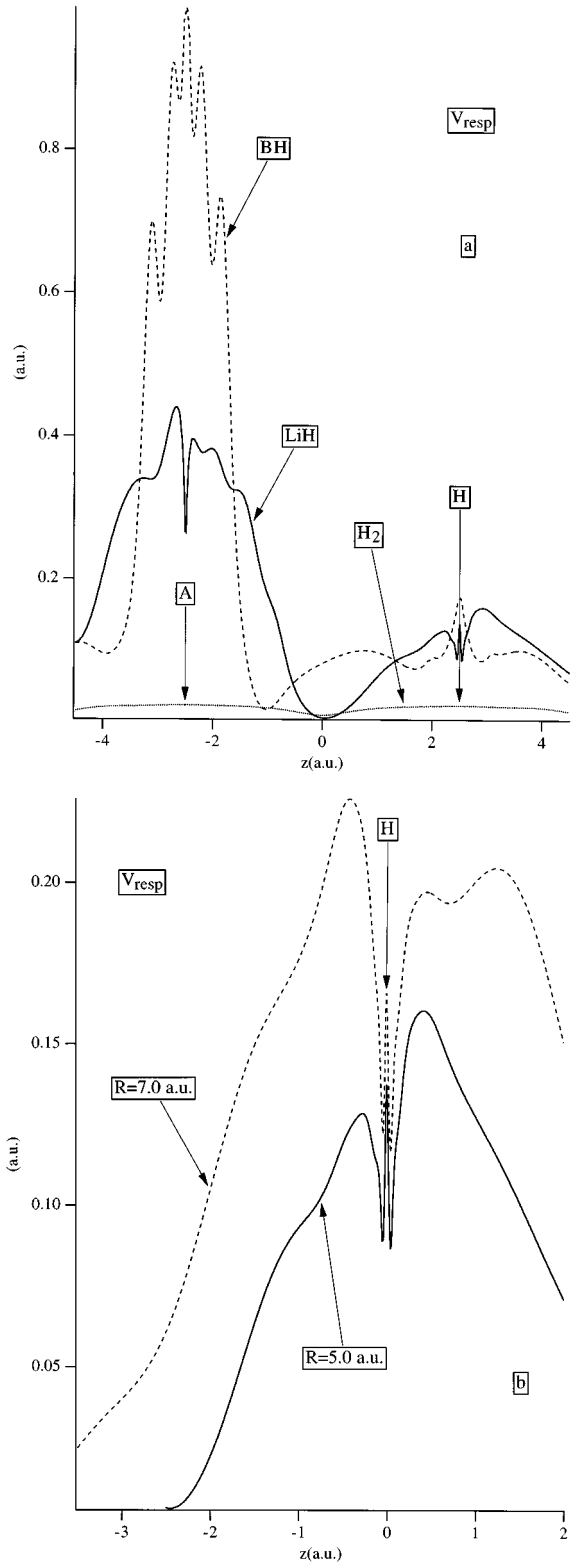

FIG. 8. Comparison of the potentials v_{resp} (a) H_2, LiH, and BH, $R=5.0$ a.u. and (b) LiH, $R=5.0$ a.u. and $R=7.0$ a.u.

$$v_{\mathrm{xc}}^{\mathrm{mod}}(\vec{r})=v_{\mathrm{xc}}^{\mathrm{hole}}(\vec{r})+K\sum_{i=1}^{N}\sqrt{\mu-\epsilon_i}\,\frac{|\phi_i(\vec{r})|^2}{\rho(\vec{r})} \qquad (72)$$

appear to be always at more negative energies than the corresponding ϵ_N values obtained with the constructed v_{xc} (the latter being presented in Tables I and II). Variation of the parameter K within reasonable limits failed to improve this deficiency.

Figure 8(a) compares the potentials v_{resp} obtained for H_2, LiH, and BH at the same elongated bond length $R=5.0$ a.u. It can serve as an illustration to the formulas (43)–(46) derived for v_{resp} in Sec. III. For both LiH and BH $v_{\mathrm{resp}}(\vec{r})$ in the region around the H atom displays the positive buildup which, according to Eqs. (43) and (45), is represented by the first three terms of Eq. (43). When the position $\vec{r}$ of the reference electron moves to the region of the HOMO near the bond midpoint $z=0$, the above-mentioned terms vanish and v_{resp} displays a minimum, which is represented by Eq. (44). When the reference electron moves further into the inner region of atom X, one has subtract from the single term of Eq. 44 the analogous contribution from v_s^{N-1} of Eq. 34. However, the energetical effect $\Delta E(A^+—B;\vec{r})$ of the electron redistribution in A^+B due to the presence of the reference electron in this inner region is much larger than that for the HOMO region and, as a result, the stepped structure of v_{resp} is created in the former region. Contrary to this, in the case of the two-electron homoatomic H_2 molecule v_{resp} is rather small everywhere and it has a flat form with very shallow maxima at the H nuclei. This flat form is anticipated, since in all regions the same formula (46) is valid for H_2.

In Fig. 8(b) v_{resp} obtained for LiH at $R=5.0$ a.u. and $R=7.0$ a.u. is plotted in the region of the H atom, the latter being placed at $z=0$. One can see from Fig. 8(b) that the positive buildup around the H atom has a similar form for both distances. In accordance with the one-dimensional model and theoretical considerations of Sec. III, the positive buildup grows higher with the increasing R and its maximum comes closer to the difference $\Delta I_p=0.302$ a.u. between the ionization energies of the H and Li atoms.

VII. CONCLUSIONS

In this paper the effect of molecular dissociation on the exchange-correlation Kohn-Sham potential v_{xc} has been established and analyzed. v_{xc} and its components have been constructed from *ab initio* correlated first- and second-order density matrices for the heteroatomic molecules LiH and BH at several bond distances $R(X—\mathrm{H})$. The results have been compared with those for the two-electron homoatomic molecule H_2.

The molecular dissociation manifests itself in the formation of a characteristic peak of v_{xc} in the bonding region. In order to interpret this behavior, a partitioning of v_{xc} has been used employing the partially integrated conditional probability amplitude $\Phi(s_1,\vec{x}_2,\ldots,\vec{x}_N|\vec{r}_1)$. This partitioning represents v_{xc} as a sum of the potential of the exchange-correlation hole $v_{\mathrm{xc}}^{\mathrm{hole}}$, the kinetic component $v_{c,\mathrm{kin}}$ and the ''response'' potential v_{resp}. For the homoatomic H_2 molecule the peak of v_{xc} is determined by the bond midpoint peak of $v_{c,\mathrm{kin}}$ (which in this case reduces to v_{kin}), while for the heteroatomic XH molecule the peak of v_{xc} is a combination of the bonding peak of $v_{c,\mathrm{kin}}$ and the positive buildup of v_{resp} around the more electronegative atom H. In all cases the peak of v_{xc} and the corresponding features of $v_{c,\mathrm{kin}}$ and v_{resp} grow higher with increasing bond distance.

It has been established, using the representation of v_{resp} in terms of the effective potential v^{N-1} of the $(N-1)$ electron system introduced in [2], that the positive buildup of v_{resp} originates from the difference between the electron distribution of $(N-1)$ electrons associated with the conditional amplitude $\Phi(s_1,\vec{x}_2,\ldots,\vec{x}_N|\vec{r}_1)$ of the heteroatomic molecule AB and that corresponding to the ground-state wave function of the cation $(AB)^+$. From the conditional amplitude analysis the asymptotical expressions for v_{resp} and its positive buildup have been obtained. The latter is represented as a leading term $[I_B-I_A]$, which arises due to the different ionization energies of atoms A and B, plus corrections due to the different polarization of A and B by a positive charge and different ''response'' of electrons of the cations $A—B^+$ and $A^+—B$ to the presence of the additional reference electron.

The dependence of the kinetic energy of noninteracting particles T_s, the kinetic part of the correlation energy T_c, and the energy of the HOMO ϵ_N on the bond distance R has been studied. In all cases T_s as a function of R passes through a minimum, while T_c and ϵ_N decreases for large R, both approaching the corresponding values for the individual atoms X. In the particular case of the H_2 molecule an accurate asymptotic formula for T_c has been obtained, according to which it approaches zero in the bond dissociation limit.

An important problem that still remains is how to increase further the numerical accuracy and stability of the molecular v_{xc} construction. As has been discussed above, construction in the finite Gaussian basis suffers from the eventual development of artificial oscillations of v_{xc} and from an inadequacy of a Gaussian basis both at nuclei and at molecular density tails. These difficulties can be, at least in principle, overcome by the construction of v_{xc} within a basis-set-free numerical molecular program. This problem, as well as the construction of v_{xc} and the exchange-correlation density ϵ_{xc} for more complex molecular processes will be addressed in our further work.

[1] D. W. Smith, S. Jagannathan, and G. S. Handler, Int. J. Quantum Chem. Quantum Biol. Symp. **13**, 103 (1979).

[2] M. A. Buijse, E. J. Baerends, and J. G. Snijders, Phys. Rev. A **40**, 4190 (1989).

[3] C. J. Umrigar and X. Gonze, Phys. Rev. A **50**, 3827 (1994).

[4] C. O. Almbladh and A. C. Pedroza, Phys. Rev. A **29**, 2322 (1984).

[5] A. C. Pedroza, Phys. Rev. A **33**, 804 (1986).

[6] F. Aryasetiawan and M. J. Stott, Phys. Rev. B **34**, 4401 (1986).

[7] F. Aryasetiawan and M. J. Stott, Phys. Rev. B **38**, 2974 (1988).

[8] Á. Nagy and N. H. March, Phys. Rev. A **39**, 5512 (1989).

[9] Y. Wang and R. G. Parr, Phys. Rev. A **47**, R1591 (1993).

[10] R. van Leeuwen and E. J. Baerends, Phys. Rev. A **49**, 2421 (1994).

[11] Q. Zhao, R. C. Morrison, and R. G. Parr, Phys. Rev. A **50**, 2138 (1994).

[12] R. C. Morrison and Q. Zhao, Phys. Rev. A **51**, 1980 (1995).

[13] O. V. Gritsenko, R. van Leeuwen, and E. J. Baerends, Phys. Rev. A **52**, 1870 (1995).

[14] V. E. Ingamells and N. C. Handy, Chem. Phys. Lett. **248**, 373 (1996).

[15] O. V. Gritsenko, R. van Leeuwen, and E. J. Baerends, J. Chem. Phys. **104**, 8535 (1996).

[16] O. V. Gritsenko, R. van Leeuwen, and E. J. Baerends, J. Chem. Phys. **101**, 8955 (1994).

[17] G. Hunter, Int. J. Quantum Chem. **9**, 237 (1975).

[18] P. Süle, O. V. Gritsenko, Á. Nagy, and E. J. Baerends, J. Chem. Phys. **103**, 10 085 (1995).

[19] M. Levy and H. Ou-Yang, Phys. Rev. A **38**, 625 (1988).

[20] M. A. Buijse and E. J. Baerends, in *Electronic Density Functional Theory of Molecules, Clusters and Solids*, edited by D. E. Ellis (Kluwer, Dordrecht, 1995).

[21] M. A. Buijse and E. J. Baerends, J. Chem. Phys. **93**, 4129 (1990).

[22] E. J. Baerends, O. V. Gritsenko, and R. van Leeuwen, in *Density Functional Methods in Chemistry*, ACS Symposium Series, edited by B. Ross, R. C. Laird, and T. Ziegler (American Chemical Society, Washington, DC, 1996).

[23] C. O. Almbladh and U. von Barth, in *Density Functional Methods in Physics*, Vol. 123 of *NATO Advanced Study Institute Series B: Physics*, edited by R. M. Dreizler and J. da Providencia (Plenum, New York, 1985).

[24] J. P. Perdew, in *Density Functional Methods in Physics* (Ref. [23]).

[25] J. B. Lagowski and S. H. Vosko, J. Phys. B **21**, 203 (1988).

[26] J. Katriel and E. R. Davidson, Proc. Natl. Acad. Sci. USA **77**, 4403 (1980).

[27] V. R. Saunders and J. H. van Lenthe, Mol. Phys. **48**, 923 (1983).

[28] G. C. Lie and E. Clementi, J. Chem. Phys. **60**, 1275 (1974).

[29] A. Savin, H. Stoll, and H. Preuss, Theor. Chim. Acta **70**, 407 (1986).

[30] M. A. Buijse, PhD thesis, Vrije Universiteit, 1991.

[31] J. C. Slater, *Quantum Theory of Molecules and Solids* (McGraw-Hill, New York, 1974), Vol. 4.

[32] A. D. Becke, Phys. Rev. A **38**, 3098 (1988).

[33] S. H. Vosko, L. Wilk, and M. Nusair, Can. J. Phys. **58**, 1200 (1980).

[34] G. te Velde and E. J. Baerends, J. Comput. Phys. **99**, 84 (1992).

[35] A. Görling, Phys. Rev. A **46**, 3753 (1992).

[36] J. P. Perdew, R. G. Parr, M. Levy, and J. L. Balduz, Phys. Rev. Lett. **49**, 1691 (1982).

[37] U. von Barth, in *The Electronic Structure of Complex Systems*, Vol. 113 of *NATO Advanced Study Institute, Series B: Physics*, edited by P. Phariseau and W. Temmerman (Plenum, New York, 1984).

[38] M. Levy, J. P. Perdew, and V. Sahni, Phys. Rev. A **30**, 2745 (1984).

[39] C. O. Almbladh and U. von Barth, Phys. Rev. B **31**, 3231 (1985).

[40] R. M. Dreizler and E. K. U. Gross, *Density Functional Theory: An Approach to the Quantum Many-Body Problem* (Springer-Verlag, Berlin, 1990).

[41] I. N. Levine, *Quantum Chemistry* (Allyn and Bacon, Boston, 1983).

[42] K. Ruedenberg, Rev. Mod. Phys. **39**, 326 (1962).
[43] M. J. Feinberg and K. Ruedenberg, J. Chem. Phys. **54**, 1495 (1971).
[44] A. Rozendaal and E. J. Baerends, Chem. Phys. **95**, 57 (1985).
[45] O. V. Gritsenko, R. van Leeuwen, E. van Lenthe, and E. J. Baerends, Phys. Rev. A **51**, 1944 (1995).
[46] J. B. Krieger, Y. Li, and G. J. Iafrate, Phys. Rev. A **45**, 101 (1992).
[47] J. D. Talman and W. F. Shadwick, Phys. Rev. A **14**, 36 (1976).
[48] K. Aashamar, T. M. Luke, and J. D. Talman, At. Data Nucl. Data Tables **22**, 443 (1978).
[49] J. D. Talman, Comput. Phys. Commun. **54**, 85 (1989).